Characterization of Gas and Particle Emissions from Open Burning of Household Solid Waste from South Africa

Xiaoliang Wang[1], Hatef Firouzkouhi[1], Judith C. Chow[1], John G. Watson[1], Warren Carter[2], Alexandra S.M. De Vos[2]

[1] Division of Atmospheric Sciences, Desert Research Institute, Reno, NV 89512, U.S.A.
[2] SASOL Research and Technology, Sasolburg, South Africa

Correspondence to: Xiaoliang Wang (xiaoliang.wang@dri.edu)

Abstract. Open burning of household and municipal solid waste is a frequent ~~common~~ practice in many developing countries. Due to limited resources for collection and proper disposal, solid waste is often disposed of in neighborhoods and open burned in piles to reduce odors and create space for incoming waste. Emissions from these ground-level and low-temperature burns cause air pollution, leading to adverse health effects among community residents. This study conducted laboratory combustion experiments to characterize gas and particle emissions from ten waste categories representative of those burned in South Africa: paper, leather/rubber, textiles, plastic bottles, plastic bags, vegetation (with three different moisture content levels), food discards, and combined materials. Carbon dioxide (CO_2) and carbon monoxide (CO) were measured in real-time to calculate modified combustion efficiencies (MCE). MCE is used along with video observations to determine fuel-based emission factors (EFs) during flaming and smoldering phases as well as the entire combustion process. Fuel elemental composition and moisture content have strong influences on emissions. Plastic bags have the highest carbon content and the highest combustion efficiency, leading to the highest EFs for CO_2. Textiles have the highest nitrogen and sulfur contents, resulting in the highest EFs for nitrogen oxides (NO_x) and sulfur dioxide (SO_2). Emissions are similar for vegetation with 0% and 20% moisture contents; however, EFs for CO and particulate matter (PM) from the vegetation with 50% moisture content are 3 and 20–30 times, respectively, those ~~emissions~~ from 0% and 20% moisture contents. This study also shows that neglecting carbon in the ash and PM can lead to significant overestimation of EFs. Results from this study are applicable to emission inventory improvements as well as air quality management to assess the health and climate effects of household waste open burning.

1 Introduction

Solid waste management is a global environmental challenge. Approximately two billion metric tons per year of ~~household and~~ municipal solid waste (MSW) are generated globally (Wilson and Velis, 2015). Even though high-income countries have higher per capita MSW generation, waste generation in middle- and low-income countries is growing rapidly due to population growth and economic development (Ferronato and Torretta, 2019). Waste disposal practices include collection, recycling, land filling, incineration, and open burning (Wilson and Velis, 2015; Wiedinmyer et al., 2014). In contrast to the near 100% collection and controlled disposal rates in high and upper-middle income countries, low-income countries often have less than 50% collection rates, with near 0% controlled disposal common in rural areas. It is estimated that at least two billion people worldwide still lack access to solid waste collection, treatment, or disposal services and infrastructure (Cook and Velis, 2021; Wilson et al., 2015).

In rural communities of developing countries, particularly regions where waste collection service is expensive, unavailable, or infrequent, uncontrolled open burning of household solid waste is a common practice for decreasing MSW mass and volume, reducing unpleasant odors from decomposing materials, fueling heating and cooking activities, and destroying pathogens (Cook and Velis, 2021). Globally, about half of the household waste (i.e., about one billion tons) is burned in open, uncontrolled fires every year. Open burning is conducted not only by community members, but also by municipal authorities.

Although perceived as a cost-effective method of waste disposal, uncontrolled solid waste open burning generates a wide range of hazardous substances that pose threats to human health and contribute to climate change (Wiedinmyer et al., 2014; Lemieux et al., 2004). These air contaminants include criteria pollutants, such as carbon monoxide (CO), nitrogen dioxide (NO_2), sulfur dioxide (SO_2), particulate matter with aerodynamic diameter ≤2.5 μm ($PM_{2.5}$) and ≤10 μm (PM_{10}), and lead. Burning also emits other air toxics, such as heavy metal elements, polycholorinated and polybrominated dioxins and furans, and polycyclic aromatic hydrocarbons (PAHs) (Velis and Cook, 2021; Wiedinmyer et al., 2014). Many of these pollutants are carcinogenic or mutagenic; they may cause immunological and developmental impairments and lead to respirable and cardiovascular diseases. It is estimated that exposure to $PM_{2.5}$ from open burning of solid waste causes at least 270,000 premature deaths in the world every year (Williams et al., 2019; Kodros et al., 2016). In addition, open burning emits large amounts of carbon dioxide (CO_2) and light absorbing carbon (including black carbon [BC]), two of the largest climate forcers to global warming (Bond et al., 2013; IPCC, 2013).

~~Several factors exacerbate the risks of open burning smoke. First, solid waste often contains fuels that release toxic compounds upon heating. For example, construction timber combustion can release high concentrations of arsenic, chromium, and copper. Plastic burning can release phthalates, PAHs, and dioxins (Velis and Cook, 2021; Wasson et al., 2005). Second, the open waste combustion temperatures are typically lower than those in controlled incinerations, resulting in lower combustion efficiencies that generate more pollutants. Even if some burns reach high temperatures, incomplete combustion is inevitable at the beginnings and ends of the burns (Cook and Velis, 2021). Third, open burning often occurs close to where people live, resulting in high exposure levels. The pollutants can be directly inhaled, distributed in the environment and subsequently ingested, or absorbed through skin.~~

Despite the global health crisis and potential climate impacts caused by uncontrolled solid waste open burning, the quantity of pollutant emissions is uncertain. Due to lack of data, household solid waste open burning emissions are not often included in regional, national, or global emission inventories (Wiedinmyer et al., 2014). Estimating household waste burning emissions faces two challenges: 1) it is difficult to estimate when, where, and how much burning occurs (activities); and 2) few ~~not many~~ studies have systematically quantified representative open burning emission factors (EFs; i.e., amount of pollutant emitted per kg of fuel burned).

Several approaches have been used to derive EFs. The Intergovernmental Panel on Climate Change (IPCC, 2006) calculates CO_2 EFs from carbon content in several categories of solid waste fuels. Bond et al. (2004) used a single PM_{10} EF ~~emission factor~~ value of 30 g kg^{-1} to represent all solid waste open burning when establishing a global inventory of black and organic carbon emissions. The U.S. Environmental Protection Agency (U.S. EPA) tested solid waste emissions when compiling and validating EFs in its AP-42 Compilation of Air Emissions Factors (U.S. EPA, 1992; Gerstle and Kemnitz, 1967; Lemieux, 1997, 1998). However, many of the fuels do not represent modern waste materials and the applied measurement technologies are outdated. Other studies acquired laboratory emissions for several waste categories, such as shredded tires, plastic bags, and mixed garbage (Stockwell, 2016; Yokelson et al., 2013; Cheng et al., 2020) and ~~. S~~several field measurements were conducted in Nepal and China (Stockwell et al., 2016; Jayarathne et al., 2018; Wu et al., 2021). ~~However, particle emissions were not often measured in these studies.~~ While EFs for biomass burning are available, data for other waste categories, particularly those in Africa, are scant (Rabaji, 2019; Kwatala et al., 2019). Developing more reliable EFs that represent open burning conditions has been identified as a research priority to reduce harm from solid waste open burning (Cook and Velis, 2021).

~~To reduce emissions and improve air quality in surrounding communities near its facilities, SASOL, a petrochemical and energy company in South Africa, is implementing a Waste Collection Interventions (WCI) program to assist the Zamdela local community in MSW collection and disposal in landfills to minimize open burning.~~ To improve emission inventories, this study conducted comprehensive laboratory combustion experiments to determine household solid waste burning emissions. The tested waste materials were collected from a Waste Collection Interventions (WCI) program implemented by SASOL, a petrochemical and energy company in South Africa, to assist the Zamdela local community in MSW collection and disposal in landfills to minimize open burning and improve air quality in communities near SASOL facilities. EFs for criterial pollutants from smoldering and flaming phases as well as the entire combustion process are reported for ten waste materials representing commonly disposed of in South Africa.

2 Method

2.1 Waste Materials

The m~~M~~ass distribution~~s~~ of common waste material categories that are burned in South Africa townships is ~~were obtained from SASOL's WCI program. As~~ shown in Fig. 1.~~,~~ ~~v~~Vegetation had the highest weight percent (33.3%), followed by plastics (20%) and paper (19.5%). Examples of major waste categories included in this study are illustrated in Supplemental Fig. S1. Due to difficulties in preserving and importing food discards ~~(organics)~~ and

vegetation, local substitutes (Nevada, USA) were used. Food waste was represented by a mixture of bread, potato and banana peels, lettuce, cucumbers, and tomatoes (Cronje et al, 2018). Vegetation samples were collected in Nevada to represent similar species in South Africa, including basin wild rye, Sandberg bluegrass, crested wheat grass, red willows, and creeping wild rye, typical of African bunch grasses, African sumac, and crab grass. EFs for glass, metals, and ceramics were not separately measured as they do not combust or degrade at open burning temperatures. However, to simulate their potential effects on combustion, these discards were included in the laboratory testing with combined waste materials. Ten types of waste categories/conditions were tested: 1) paper; 2) leather/rubber; 3) textile; 4) plastic bottles and food containers (hard plastics); 5) plastic bags (soft plastics); 6) dry vegetation (0% moisture content); 7) natural vegetation (20% moisture content); 8) damp vegetation (50% moisture content); 9) food discards; and 10) combined materials. The combined materials were mixtures of all ~~the other~~ categories based on their mass fractions in Fig. 1. Each category was tested at least three times, except that the vegetations with 20% and 50% moisture content were each tested twice.

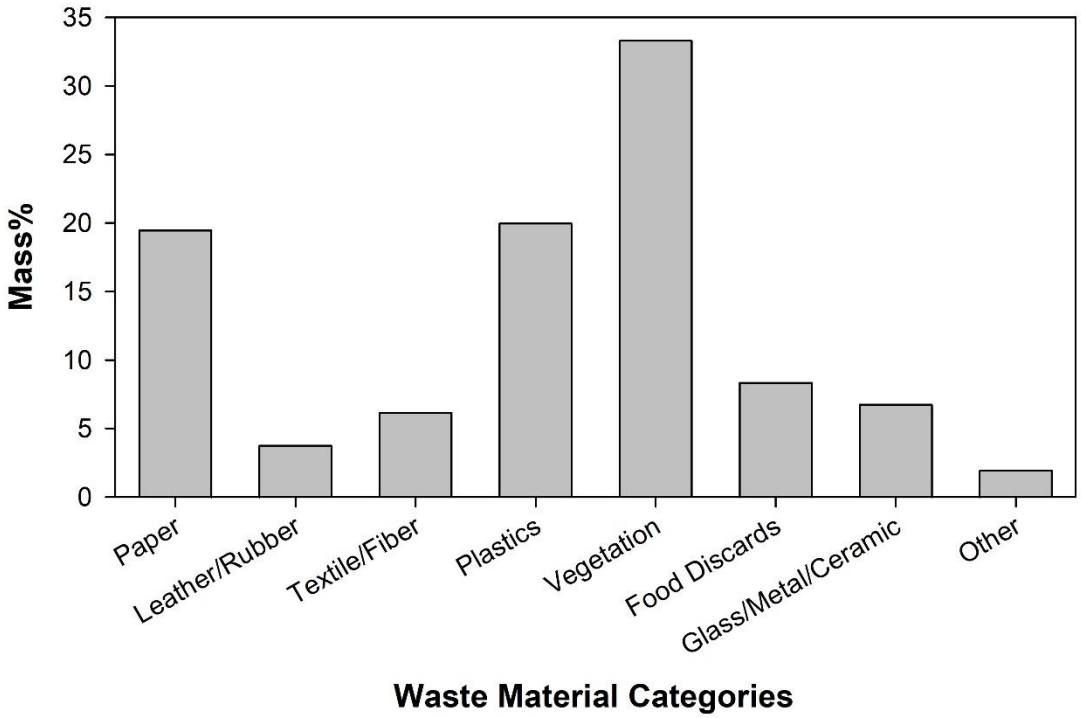

Figure 1: Mass fraction of municipal solid waste categories collected by Sasol's Waste Collection Interventions (WCI) program in Zamdela, South Africa.

Because fuel moisture content affects combustion behavior and emissions (Rein et al., 2008; Chen et al., 2010), the moisture contents of waste materials were measured right after field collection, ranging 0.5–35% (Table S1~~Table S1~~). To account for moisture changes during shipping and storage, all materials (except food discards) were oven dried at 90 °C for 24 hours. A calculated amount of distilled deionized water (DDW) was then added to the dried materials to achieve the natural moisture levels shown in Table S1~~Table S1~~. These moisturized materials were sealed in airtight bags to equilibrate for at least 24 hours before testing. Fresh food discards were tested without drying/re-moisturizing to avoid irreversible changes. The moisture content for the combined waste was calculated as the sum of the mass-weighed moisture content in individual waste category.

Table S2~~Table S2~~ shows the major elemental compositions (i.e., carbon [C], hydrogen [H], nitrogen [N], sulfur [S], and oxygen [O]) of the waste materials measured by an elemental analyzer (Model Flash EA1112, Thermo Scientific). Plastic bags (84%) and plastic bottles (64%) have higher carbon contents than other materials (33–48%). ~~The carbon content is used for the fuel-based EF calculation.~~ These ~~C%~~carbon contents fall within the IPCC (2006) range for all materials except the leather/rubber category: 33% (this study) vs. 67% (IPCC, 2006). The single synthetic leather/rubber piece (a car floor mat) measured in this study may not be representative of all such materials available elsewhere. Unlike other waste categories, IPCC (2006) does not give a range of carbon content ~~C%~~ for leather/rubber, indicating a need for a wider range of testing for this category.

The textile category contained the highest nitrogen (8%) and sulfur (0.71%) contents, while most other materials yielded sulfur contents below the minimum detection limit. The paper category had the highest oxygen content (44%), followed by vegetation and food discards (41–42%). The lowest (~3%) oxygen was found for soft plastic bags.

After combustion, the ash was weighed to calculate its mass fraction related to the original dry material mass, ranging from 2% to 58% (Table S3~~Table S3~~). The C, H, N, and S content of the ash was also measured by the elemental analyzer, and the ash carbon content ~~C% is~~ was used in the EF calculation.

2.2 Combustion Experiments

The experimental setup is shown in Fig. 2, similar to the ones used in previous studies (Chen et al., 2010; Chow et al., 2019; Tian et al., 2015; Wang et al., 2019, 2020b). Key specifications for gas and particle measurement instruments are listed in Table S4~~Table S4~~. For each experiment, a small amount (0.5 – 20 g) of waste material was placed in a ceramic crucible inside a woodstove, then quickly heated to and maintained at 450 °C by a temperature-controlled heater to simulate large scale open burning. The heater accounts for open burning temperatures surrounding the fuel materials that could be much higher than those produced by laboratory fuels (Chen et al., 2010; Chow et al., 2019). Flammable waste materials (i.e., paper, textile, plastic bags, dry and natural moist vegetations, and combined wastes) were ignited by an electric heat gun or a butane lighter. For nonflammable materials ~~Smoldering emissions were measured for non-flammable materials~~ (i.e., leather/rubber, plastic bottles, damp vegetation, and food discards), smoldering emissions were measured when the materials were heated to 450 °C. Each test started with about 5-minute sampling of background concentrations and ended when ~~until the~~ pollutant concentrations returned to baselines. Elapsed time varied from 1000 to 4000 s for each burn, with typical run times of 30 min per sample. An exhaust fan drew fresh air through the stove inlet and vented the smoke above the roof via the stack. Temperature and relative humidity (RH) of the exhaust air were monitored by a hygrometer (Model HH314A, Omega). A web camara inside the stove recorded the combustion process.

During combustion, major fuel components of C, H, N, and S are oxidized to generate carbon dioxide (CO_2), carbon monoxide (CO), water (H_2O), oxides of nitrogen (NO_x), sulfur dioxide (SO_2), volatile organic compounds (VOCs), and particulate matter (PM) (Akagi et al., 2011). The air sample was extracted from the stack through a sampling line and directed to a suite of gas and particle analyzers (Table S4~~Table S4~~). CO_2 was measured by a CO_2 analyzer (Model 840A; Li-Cor). CO was measured by a CO analyzer (Model 48i, ThermoFisher Scientific), which is designated as a federal equivalent method (FEM) by the U.S. Environmental Protection Agency (U.S. EPA). ~~CO and~~

~~CO_2 concentrations were used to calculate the modified combustion efficiency (MCE) and fuel based EFs.~~ SO_2 was measured by a FEM SO_2 analyzer (Model 43i, ThermoFisher Scientific). Nitric oxide (NO), nitrogen dioxide (NO_2), and NO_x were measured by a FEM $NO/NO_2/NO_x$ analyzer (Model APNA-360, Horiba Ltd). An emission analyzer (Model 350 XL, Testo Inc.) provided redundant measurements of CO_2, CO, SO_2, NO, and NO_2, in order to accommodate high concentrations in the event that the FEM analyzers were saturated. In addition, the Testo also measured oxygen (O_2), temperature (T), and pressure (P). Size segregated PM mass concentrations were acquired every second by an aerosol monitor (Model DustTrak DRX, TSI Inc.) in five size fractions (i.e., PM_1, $PM_{2.5}$, PM_4, PM_{10}, and PM_{15}) (Wang et al., 2009). Gas and particle analyzers were calibrated before and after experiments. All analyzer responses were quality checked to ensure readings were within their measurement ranges.

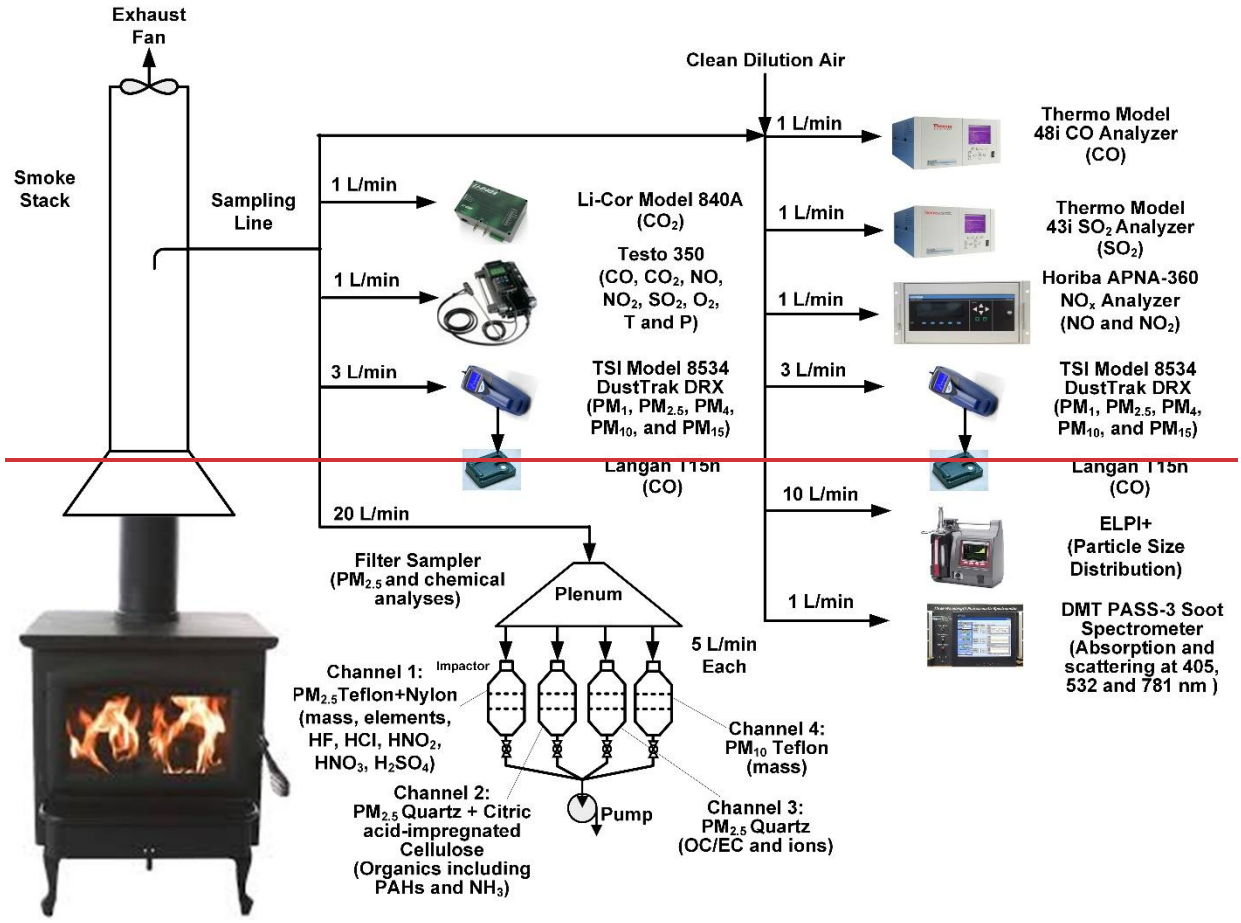

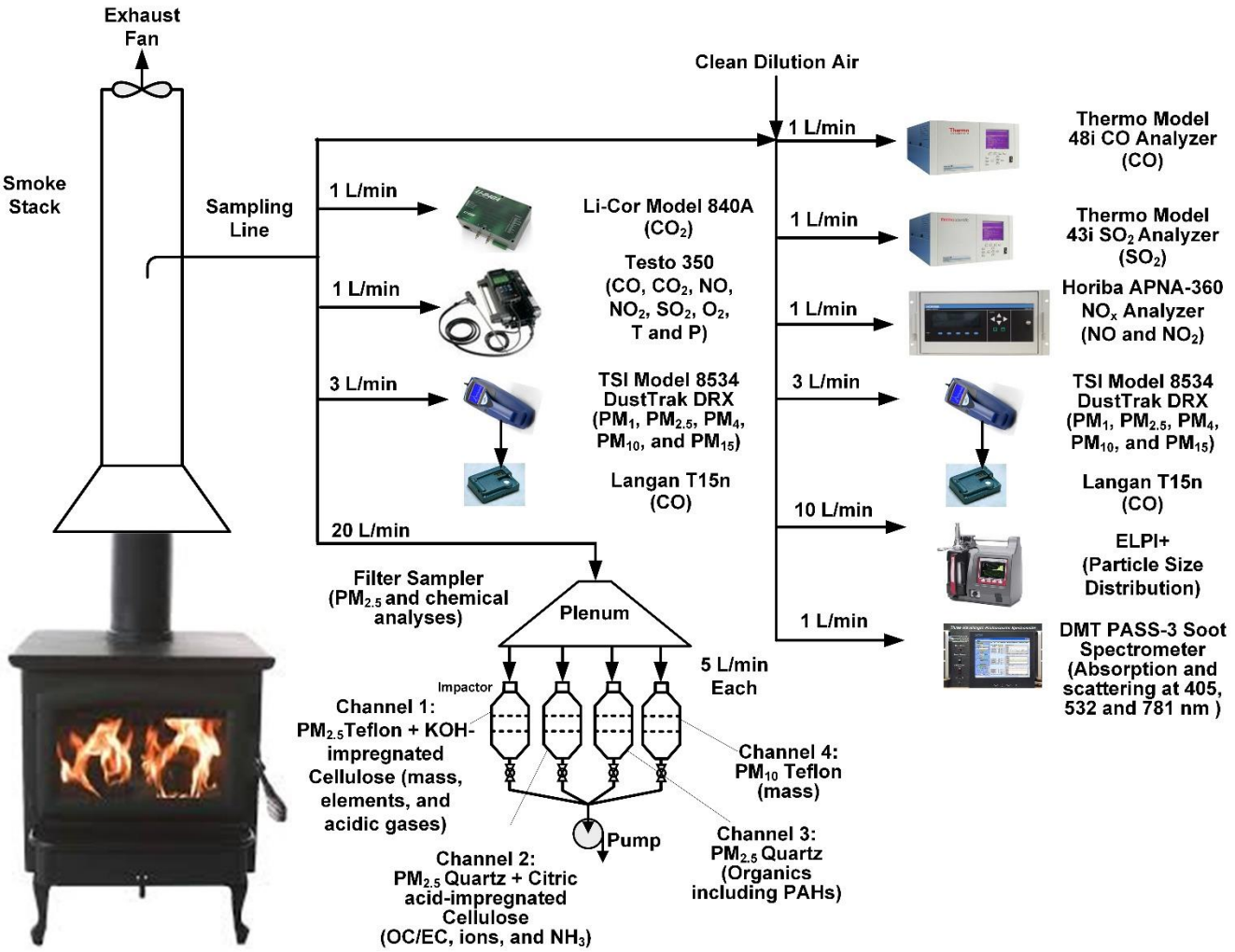

Figure 2: Experimental setup for solid waste combustion.

$PM_{2.5}$ and PM_{10} samples were collected on Teflon-membrane and quartz-fiber filters. The gravimetric mass concentrations were used to calibrate the real-time mass concentrations by the DRX. Organic and elemental carbon (OC and EC) were analyzed from the quartz-fiber filters using the DRI Model 2015 Multiwavelength Carbon Analyzer following the IMPROVE_A protocol (Chow et al., 2007; Chen et al., 2015). ~~The filters were also analyzed for~~ ~~d~~Detailed chemical composition of $PM_{2.5}$ ~~,~~analyzed from the filters, particle size distribution by the Electrical Low Pressure Impactor ($ELPI^+$), and particle light scattering and absorption by the Photoacoustic Soot Spectrometer (PASS-3) ~~which~~ will be reported in ~~a~~ future publications.

2.3 Data Analysis

Data from real-time gas and particle analyzers were assembled and mapped to a common time stamp with one-second time resolution. Time series of gas and particle concentrations were aligned to account for their different transport and response times. Calibration factors were applied to each analyzer. Modified combustion efficiency (MCE) was calculated as

$$MCE = \frac{\Delta CO_2 \Delta CO2}{\Delta CO_2 \Delta CO2 + \Delta CO} \quad (1)$$

where ΔCO_2 and ΔCO are CO_2 and CO concentrations above background concentrations. MCE provides a real-time indicator of the combustion phase (i.e., MCE ≥ ~0.9 for flaming and MCE < 0.9 for smoldering) (Reid et al., 2005; Yokelson et al., 1996; Wang et al., 2020a).

Fuel-based emission factors ($EF_{p,i}$) were calculated based on carbon mass balance techniques as (Wang et al., 2019; Chen et al., 2007; Moosmüller et al., 2003):

$$EF_{p,i} = \left(CMF_{fuel} - \frac{m_{ash}}{m_{fuel}} CMF_{ash}\right) \frac{C_p}{C_{CO_2}\left(\frac{M_C}{M_{CO_2}}\right) + C_{CO}\left(\frac{M_C}{M_{CO}}\right) + C_{PM}} \times 1000 \quad (2)$$

where $EF_{p,i}$ is the emission factor of pollutant p from waste material i in g per kg of fuel. CMF_{fuel} is the carbon mass fraction of the fuel in g carbon per g of fuel (Table S2Table S2), and CMF_{ash} is the carbon mass fraction of the ash in g carbon per g of ash (Table S3Table S3). m_{ash} and m_{fuel} are the mass of ash and fuel in g, respectively. C_p is the mean plume concentration of pollutant p in g m^{-3} averaged over the calculation period (i.e., flaming, smoldering, or entire combustion process); and C_{CO} and C_{CO_2} are the mean concentrations of CO_2 and CO in g m^{-3}, respectively. C_{PM} is the mean total carbon (TC = OC + EC) concentration in PM_{10} in g m^{-3}. M_C, M_{CO_2CO2} and M_{COCO} are the atomic or molecular weights of carbon, CO_2, and CO in g per mole, respectively. The factor of 1000 converts mass from kilograms to grams. Eq. (2) assumes that the carbon mass in emissions other than CO_2, CO, and PM_{10} is negligible, which is a reasonable assumption for such burns. However, it is recognized that some carbon will be emitted as methane (CH_4) and VOCs, causing the EFs determined by Eq. (2) slightly overestimated. For waste materials that had both flaming and smoldering combustions, the split points between the two phases were determined from the burn video recording and MCE. $EF_{p,i}$ for flaming, smoldering, and the entire burning process were calculated. Means and standard deviations of $EF_{p,i}$ for each waste category and/or burn condition were calculated from repeated tests.

3 Results and Discussion

3.1 Evolution of Air Pollutants during Combustion

Time series plots of criteria pollutant concentrations, along with photographs of the waste materials, ash, and sample filters for each waste category are presented in Supplementary Section S3 to provide more details on the emission evolution, flaming vs. smoldering phases, ash contents, and potential light absorption properties for each fuel. Results for plastic bottles and bags are presented below to illustrate experimental findings from smoldering- and flaming-dominated combustions, respectively.

Trial burns with ~5 g of mixed plastic bottles generated very high PM concentrations that clogged filters and overloaded real-time particle sampling instruments. The final tests for this fuel utilized 0.5 g of this material moisturized to 0.54% water content (Fig. S13a). As shown in Fig. 3, smoldering started ~100 s after initial heating with low CO_2 and CO concentrations. PM emissions were the highest among all the waste materials, likely formed from re-condensation of semivolatile thermal decomposition products, such as carboxylic acids and hydroxyl esters including phthalates (Sovová et al., 2008; Holland and Hay, 2002) evaporated plastic molecules. The MCE was only

~0.6 during most duration of the burn, indicating low combustion efficiencies. NO_x concentrations were only slightly above the ~~close to~~ background levels during the peak emission period, likely due to the low combustion temperatures, ~~and~~ low nitrogen content of the plastic bottles~~fuel~~ (Table S2~~Table S2~~), and a small quantity of materials burned.

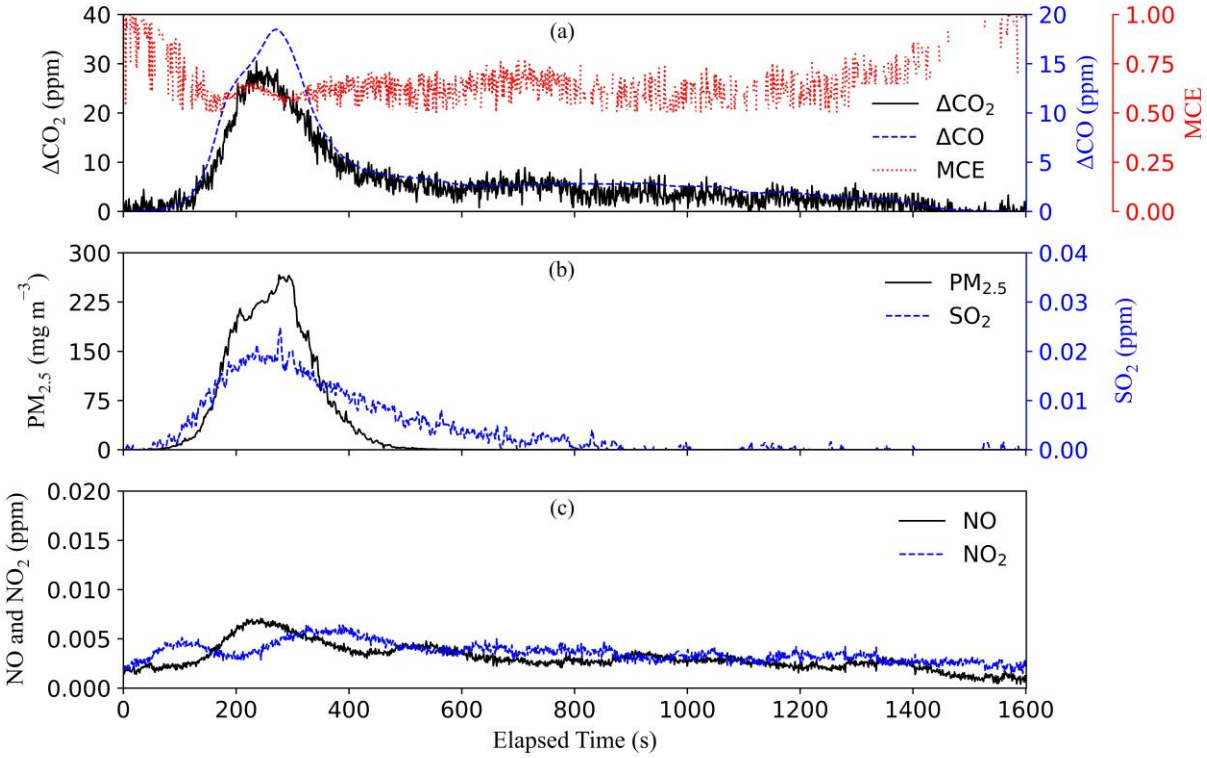

Figure 3: Time series of emissions during a plastic bottle burning experiment.

For the plastic bag experiment, 5 g of mixed soft plastic bags (Fig. S16a) were prepared with 0.54% moisture content. Flaming started at ~150 s after ignition, causing all pollutant concentrations to increase (Fig. 4). In contrast to the smoldering-only plastic bottle combustion, flaming dominated the soft plastics combustion, generating ~20 times higher CO_2 and CO concentrations. The shaded area in Fig. 4 shows the period during which flame was visible from the video camera. The MCE was high (> 0.94) during most parts of burn, indicating high combustion efficiencies. Plastic bags produced the highest CO_2 and the lowest CO EFs among all test materials, consistent with the high MCEs due to their high C and H content (Table S2~~Table S2~~). Due to the higher combustion temperatures, NO_x concentrations during plastic bag burning were also higher than those in plastic bottles burning. Only a small amount of ash (3.4%) remained after combustion (Fig. S16b).

Among the ten waste types, paper, textile, soft plastic bags, vegetations with dry and natural moisture contents, and combined waste had both flaming and smoldering phases. Leather/rubber, plastic bottles, damp vegetation, and food discards only smoldered. Ash residues were the highest for rubber (~58%) (Table S3~~Table S3~~), consistent with its high fraction of elements other than C, H, N, S, and O (Table S2~~Table S2~~). Similar flaming-dominated burns were found for vegetations with 0% and 20% moisture content (Figs. S20 and S21),~~.~~ ~~I~~in contrast to the smoldering dominated 50% moist vegetation that charred but did not flame (Fig. S22). The mean MCEs for 0%, 20%, and 50%

moisture content vegetations were ~0.92, 0.9, and 0.8, respectively, signifying the role of the moisture in the combustion efficiency (Chen et al., 2010).

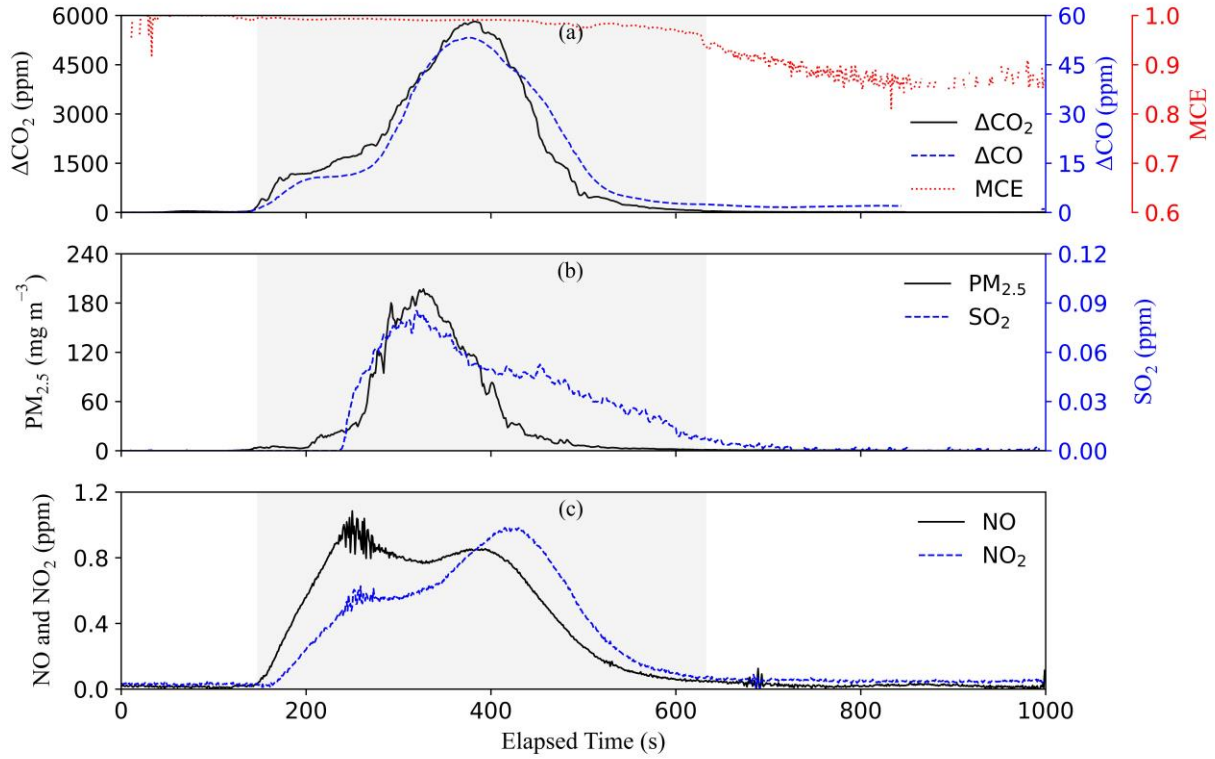

Figure 4: Time series of emissions during a plastic bag burning experiment. The shaded areas indicate flaming stage.

3.2 $PM_{2.5}$, PM_{10}, and Particulate Carbon

Figure 5~~Figure 5~~ shows high correlations (R^2 = 1) between $PM_{2.5}$ and PM_{10} mass for 30 sample sets. The linear regression slopes indicate that $PM_{2.5}$ constituted ~93% of PM_{10}, consistent with findings for ~~other~~ combustion emissions reported in the literature (e.g., U.S. EPA, 1992; Lemieux, 1997).

Since the DRX measures PM concentration based on light scattering and its conversion from the scattering signal to mass concentration depends on particle refractive index, density, and size distribution, the DRX concentrations need to be calibrated with gravimetric concentrations (Wang et al., 2009). The mean DRX and gravimetric $PM_{2.5}$ and PM_{10} mass concentrations are highly correlated with R^2 of 0.95–0.96 (Fig. S2). The DRX measured mass concentrations ~~with standard calibration~~ were about twice of those by gravimetry (slopes of 1.88 for $PM_{2.5}$ and 1.82 for PM_{10}). The DRX had an internal custom photometric calibration factor (PCF) of 1.0 and size calibration factor (SCF) of 1.7. The higher DRX reported concentrations are expected because the standard calibration uses Arizona Road Dust (ARD) with a density of 2.65 g cm^{-3} (Wang et al., 2009) while the major compositions of the combustion particles are OC and EC, which have lower densities (~1.8 and 1.1–1.4 g cm^{-3}, respectively) (Schmid et al., 2009). The DRX concentrations are normalized to the gravimetric $PM_{2.5}$ and PM_{10} concentrations for EF calculations.

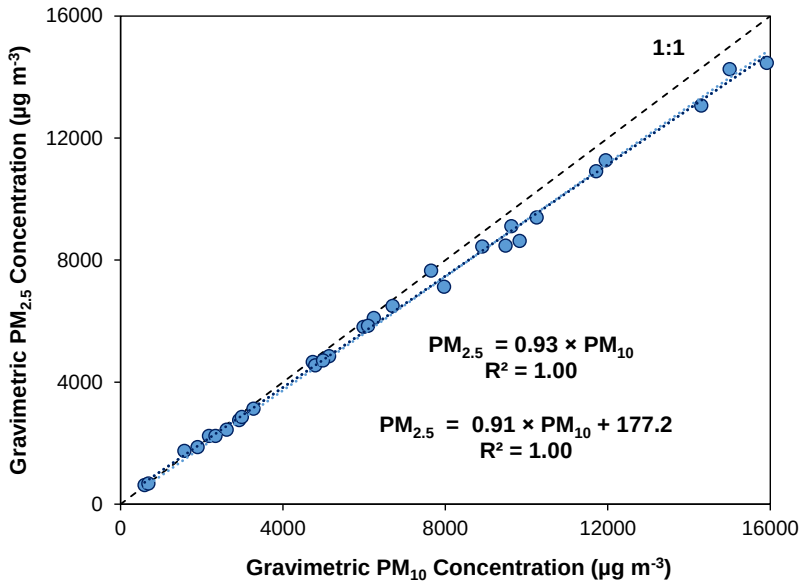

Figure 5: Comparison of $PM_{2.5}$ and PM_{10} mass concentrations measured from the Teflon-membrane filters.

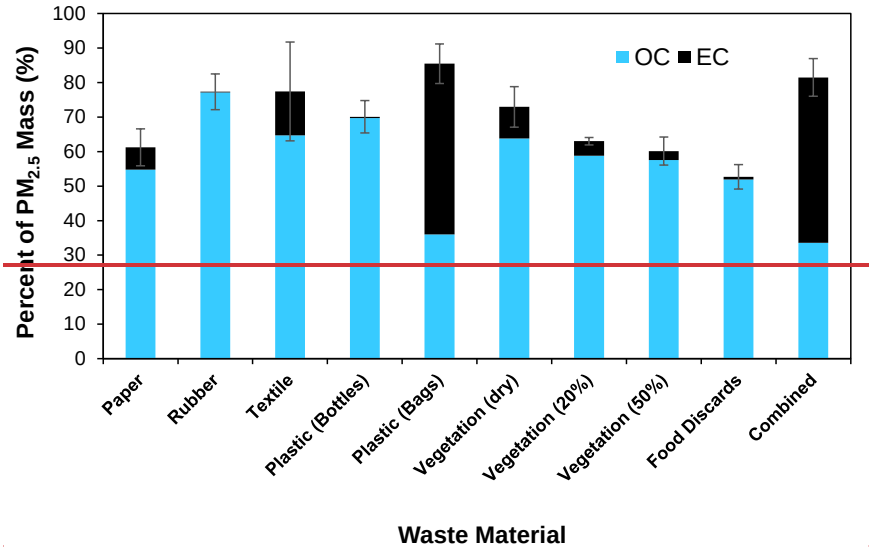

Carbon is the most abundant $PM_{2.5}$ component. As shown in Fig. 6, TC contributed 70±11% (ranging 51–94%) of $PM_{2.5}$ mass ~~emissions~~, with higher OC found in smoldering dominated materials (i.e., rubber, plastic bottles, damp vegetation, and food discards). The EC fraction increased during flaming combustion, particularly for plastic bags and combined materials. Since PM_{10} is only ~7% higher than $PM_{2.5}$ (Fig. 5), it is reasonable to assume that $PM_{2.5}$ and PM_{10} have comparable TC fractions. The C_{PM} in Eq. (2) was calculated from the TC fraction in $PM_{2.5}$ (Fig. 6) multiplied by the PM_{10} mass concentration.

The properties and abundances of OC and EC affect the optical properties of PM emissions. Photographs of sample filters in the insert of Fig. 6 and in Section S3 show that particles from flaming-dominated combustion of textiles, plastic bags, and combined materials have grey to black coloration due to high EC abundances. Some OC-abundant filters do not show colors (e.g., rubber and plastic bottles) or show yellow/brown colors (e.g., paper, damped

vegetation, and food discards), suggesting the presence of different amount of brown carbon (Andreae and Gelencsér, 2006; Chen et al., 2021). Quantitative analysis of particle optical properties will be reported in a separate publication.

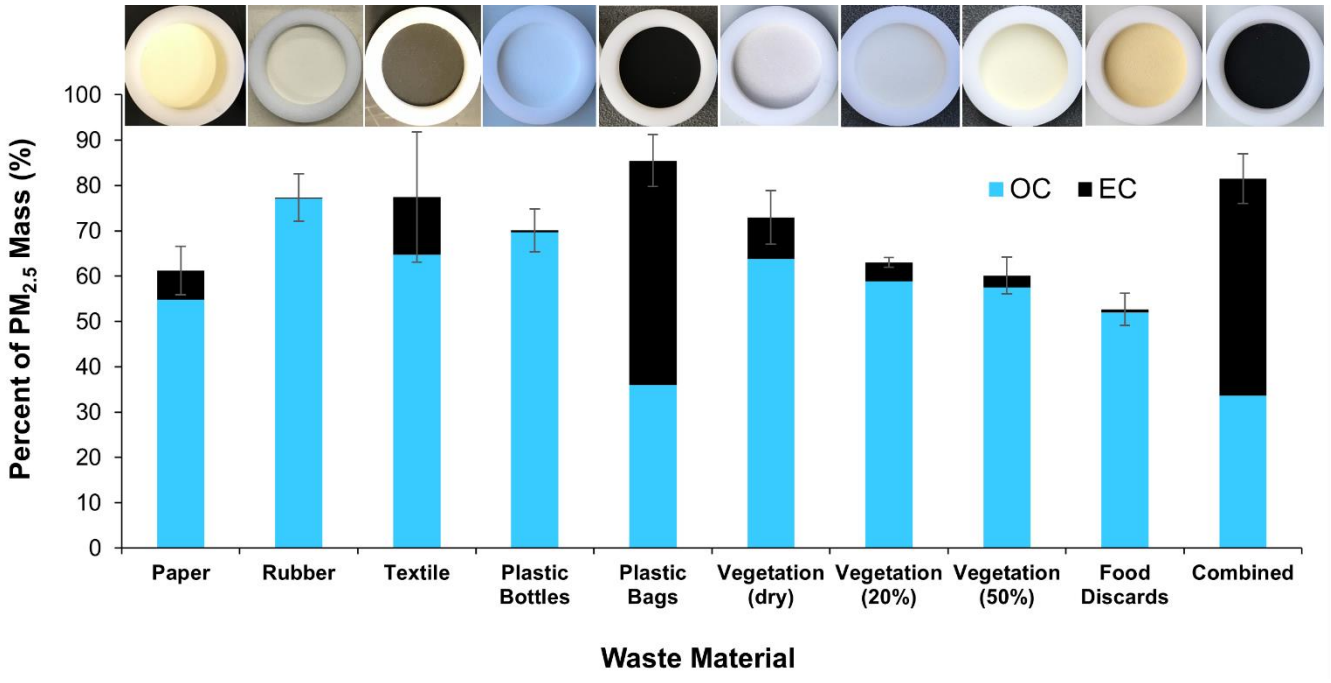

Figure 6: Mass percent of organic carbon (OC) and elemental carbon (EC) in $PM_{2.5}$. The error bar indicates the uncertainty of total carbon (TC = OC + EC), calculated as the larger of the analytical uncertainty and standard deviation of multiple runs. The top row insert shows photographs of representative $PM_{2.5}$ quartz-fiber filters collected from burning of each material.

3.3 Emission Factors (EF) for Criteria Pollutants

The percentages ~~fractions~~ of consumed waste materials and emissions during flaming and smoldering phases for each category are listed in Table 1~~Table 1~~. Mean EFs for criteria pollutants are reported in Table 2~~Table 2~~ for flaming and smoldering phases, as well as for the entire combustion process. The relative standard deviations (RSD) of total EFs from multiple tests of each material were within 50% of the mean, showing ~~confirming~~ reproducibility. Except for plastic bags that have high EFs due to high carbon fuel content, total CO_2 ~~and CO~~ EFs are relatively consistent for materials that have both flaming and smoldering phases (i.e., paper, textile, dry and natural vegetation, and combined waste), with an RSD of 3% ~~and 25%~~and an ANOVA test p-value of 0.20~~, respectively~~, in part due to similar fuel carbon contents as shown in Table S2~~Table S2~~ (RSD = 6%). Several exceptions with high RSD (e.g., NO_x for textile and plastic bottles) were due to fuel material heterogeneity or low emission levels. The RSD for the flaming phases and smoldering phases were higher than those for the entire burns due to a somewhat subjective split between the two phases. Table 3~~Table 3~~ compares EFs from this study with those reported in the literature for similar fuel materials.

For paper, most of the fuel (76%) was consumed in the flaming phase (Table 1~~Table 1~~), consistent with elevated CO_2 concentrations (Fig. S4). Approximately 65–85% of pollutants were emitted in the flaming phase except for CO, which was emitted about equally in both phases. EFs for CO in the smoldering phase were ~4 times of those in flaming phase. EFs for paper combustion are scarce in the literature (Table 3~~Table 3~~). Results from this study are close to these reported by Cheng et al. (2020). The EFs for $PM_{2.5}$ and PM_{10} are higher than other studies; ~~reported by~~ Park et al.

(2013) reported~~were~~ an order of magnitude lower EFs than ~~those from~~ this study. Paper briquettes used in the Marshall Islands (Thai et al., 2016; Xiu et al., 2018) likely have different combustion behaviors compared to the open burning of loose paper; therefore, and the EFs are not considered to be comparable.

The car floor mat synthetic rubber sample only smoldered without flaming, leading to low CO_2 and high PM EFs (Table 2~~Table 2~~). A large fraction (58%) of material was unburned as ash with a 13% carbon content (Table S3~~Table S3~~). Field and laboratory studies of tire burning emissions (Ryan, 1989; Downard et al., 2015; Stockwell, 2016) report higher EFs than those found here for most pollutants, but PM_{10} EFs are similar.

Textile burning consumed 78% of the mass and emitted 60–90% pollutants in the flaming phase except for ~20% more CO emissions in the smoldering phase (Table 1~~Table 1~~). While EFs for CO_2 and SO_2 were higher in the flaming phase, EFs for CO and PM were higher in the smoldering phase (Table 2~~Table 2~~). Textile burning had the highest EFs for NO_x and SO_2 among all tested materials, consistent with higher nitrogen and sulfur contents (Table S1~~Table S1~~). Wesolek and Kozlowski (2002) measured gas emissions during thermal decomposition of natural and synthetic fabrics at 450, 550, and 750 °C. The EFs for CO_2 and CO from this study fall within the ranges of those reported for different fabrics (Table 3~~Table 3~~). EFs for NO_x and SO_2 are~~were~~ higher in this study, likely due to differences in material compositions. EFs from this study are also higher than those reported by Cheng et al. (2020).

The plastic bottles only smoldered, yielding the lowest CO_2 EFs and among the highest CO and PM EFs (Table 2~~Table 2~~). Most fuel carbon was turned into PM and volatile organics (strong odor). In contrast, flaming dominated plastic bag combustion, consuming ~99% of the fuel mass and contributing to over 90% of emissions (Table 1~~Table 1~~). Among all waste materials, plastic bags had the highest CO_2 EFs due to their high carbon content (Table S1~~Table S1~~) and high combustion efficiencies. Similar high efficiency combustion of plastic bags is reported by Stockwell (2016). Plastic bag EFs are~~were~~ in the same range as literature values. Note that the literature has a wide range of PM EFs (Table 3~~Table 3~~), likely due to different plastic materials and burning conditions ~~(Table 3)~~ (Park et al., 2013; Lemieux et al., 2004; Oberacker et al., 1992; Stockwell et al., 2016; Jayarathne et al., 2018; Stockwell, 2016; Wu et al., 2021).

The flaming phase for vegetations with 0% and 20% moisture content consumed ~70% of the fuel mass and emitted over 70% of pollutants, except that ~60–75% of the CO was emitted during smoldering (Table 1~~Table 1~~). The damp 50% moisture content vegetation emitted 26% less CO_2, but a factor of 3 and 20–30 higher CO and PM, respectively, as compared to the drier vegetations. Most of the published vegetation emissions lack information on moisture content. Some studies with fuels relevant to South Africa are compared in Table 3~~Table 3~~ (Christian et al., 2010; Akagi et al., 2011; Santiago-De La Rosa et al., 2018; Yokelson et al., 2009; Ni et al., 2015; EMEP/EEA, 2019). The EFs are consistent with those of low moisture contents measured in this study. In particular, EFs for CO_2, CO, and SO_2 derived here are in good agreement with those derived for Savanna vegetation (Akagi et al., 2011). The EFs for PM from damp vegetation burning were about one order of magnitude higher than literature values.

Food discards did not flame due to high moisture contents in fresh vegetables and fruits, resulting in lower EFs for CO_2 and higher EFs for CO and PM (Table 2~~Table 2~~). Food discards are often included in municipal/household waste, but no separate EFs for food discard burning have been found in the literature.

Flaming-dominated combustion of the combined materials consumed 81% of the fuel mass and emitted over 75% of the pollutants, except that 62% of the CO was emitted during smoldering (Table 1~~Table 1~~). Combined waste combustion was efficient and MCE for most of the burn period was higher than 0.90 (Fig. S29). The EFs for combined waste fall within the EF ranges of the individual waste categories, but with lower EFs for PM (Table 2~~Table 2~~). Considering the wide variety of waste materials and burn practices, EFs are expected to vary over a wide range. Interestingly, as shown in Table 3~~Table 3~~, with the exception of an old (1967) test in the USA (U.S. EPA, 1992; Gerstle and Kemnitz, 1967) with a "below average" data quality rating and the study by Park et al. (2013) which showed consistently lower EFs than other studies, most ~~recent~~ other studies show reasonable consistency in EFs (Lemieux, 1997, 1998; Christian et al., 2010; Stockwell et al., 2016; Jayarathne et al., 2018; Akagi et al., 2011; Reyna-Bensusan et al., 2018; Wiedinmyer et al., 2014; Yokelson et al., 2013; Stockwell, 2016; Cheng et al., 2020). EFs for CO_2 and CO from this study agree remarkably well with data suggested for global emission inventory development (Akagi et al., 2011; Reyna-Bensusan et al., 2018; Wiedinmyer et al., 2014).

Table 2~~Table 2~~ shows that CO_2 EFs are 10–25% higher for flaming compared to smoldering and are lowest for smoldering only combustions, while CO EFs are 4–9 times higher for smoldering than for flaming. Figure S3~~Figure S3~~a and b show that overall, CO_2 increased with MCE while CO decreased with MCE, although there were large variations among fuel materials. Among the tested materials, textile has the highest nitrogen and sulfur contents, resulting in the highest EFs for NO_x and SO_2. EFs for NO_x are generally higher in the smoldering phase (except for vegetation), probably due to the time required for fuel nitrogen to be oxidized and released. Due to larger fuel influences, NO_x emissions do not show a strong pattern as a function of MCE (Fig. S3c). EFs for SO_2 are generally higher in the flaming phase (except for plastic bags). Figure S3~~Figure S3~~d shows that EFs for $PM_{2.5}$ do not show a strong correlation with MCE. Over two-fold higher EFs are found in smoldering than flaming of textile and plastic bags, with less variations between the two phases for paper, vegetation, and combined materials (Table 2~~Table 2~~).

Table 1: Percentage of consumed fuel and emissions during flaming and smoldering phases.

Fuel	Burn Type	Relative Fraction of Fuel Burned and Emissions in Flaming and Smoldering Phases (%)								
		Burned Fuel Mass	CO_2	CO	NO	NO_2	NO_x	SO_2	$PM_{2.5}$	PM_{10}
Paper	Flaming	76 ± 8	77 ± 7	46 ± 18	72 ± 12	64 ± 16	68 ± 14	84 ± 5	69 ± 22	69 ± 22
	Smoldering	24 ± 8	23 ± 7	54 ± 18	28 ± 12	36 ± 16	32 ± 14	16 ± 5	31 ± 22	31 ± 22
Leather/ Rubber	Flaming	No Flaming Phase								
	Smoldering	100								
Textile	Flaming	78 ± 8	81 ± 6	41 ± 19	75 ± 19	76 ± 18	75 ± 19	90 ± 2	61 ± 23	60 ± 23
	Smoldering	22 ± 8	19 ± 6	59 ± 19	25 ± 19	24 ± 18	25 ± 19	10 ± 2	39 ± 23	40 ± 23
Plastic Bottles	Flaming	No Flaming Phase								
	Smoldering	100								
Plastic Bags	Flaming	99 ± 0	99 ± 0	93 ± 2	96 ± 2	93 ± 2	94 ± 2	96 ± 2	97 ± 3	97 ± 3
	Smoldering	1 ± 0	1 ± 0	7 ± 2	4 ± 2	7 ± 2	6 ± 2	4 ± 2	3 ± 3	3 ± 3
Vegetation (0% mc*)	Flaming	72 ± 4	75 ± 4	26 ± 1	80 ± 3	77 ± 5	80 ± 3	94 ± 1	87 ± 8	87 ± 8
	Smoldering	28 ± 4	25 ± 4	74 ± 1	20 ± 3	23 ± 5	20 ± 3	6 ± 1	13 ± 8	13 ± 8
Vegetation (20% mc*)	Flaming	70 ± 3	72 ± 1	43 ± 18	77 ± 0	81 ± 1	79 ± 0	94 ± 2	91 ± 4	91 ± 4
	Smoldering	30 ± 3	28 ± 1	57 ± 18	23 ± 0	19 ± 1	21 ± 0	6 ± 2	9 ± 4	9 ± 4
Vegetation (50% mc*)	Flaming	No Flaming Phase								
	Smoldering	100								
Food Discards	Flaming	No Flaming Phase								
	Smoldering	100								
Combined	Flaming	81 ± 0	83 ± 1	38 ± 2	75 ± 2	83 ± 3	78 ± 2	97 ± 1	82 ± 8	82 ± 8
	Smoldering	19 ± 0	17 ± 1	62 ± 2	25 ± 2	17 ± 3	22 ± 2	3 ± 1	18 ± 8	18 ± 8

*mc: fuel moisture content

Table 2: Measured emission factors (mean ± standard deviation) for waste materials tested in this study.

Fuel	Burn Type	Mean MCE	Emission Factor (g kg^{-1} fuel)							
			CO_2	CO	NO (as NO_2)	NO_2	NO_x (as NO_2)	SO_2	$PM_{2.5}$	PM_{10}
Paper	Flaming	0.96 ± 0.03	1530 ± 24	26.2 ± 6.9	0.58 ± 0.04	0.42 ± 0.15	1.00 ± 0.15	0.68 ± 0.58	12.05 ± 3.28	12.19 ± 3.70
	Smoldering	0.87 ± 0.04	1406 ± 22	101.2 ± 13.3	0.81 ± 0.51	0.86 ± 0.53	1.66 ± 1.00	0.33 ± 0.08	15.21 ± 6.96	15.16 ± 6.67
	Total	0.90 ± 0.02	1498 ± 7	44.9 ± 3.2	0.63 ± 0.16	0.52 ± 0.19	1.14 ± 0.31	0.57 ± 0.41	13.31 ± 0.77	13.42 ± 1.21
Rubber	Flaming		No Flaming Phase							
	Smoldering	0.92 ± 0.02	456 ± 41	28.1 ± 3.9	0.31 ± 0.15	2.75 ± 4.44	3.06 ± 4.59	0.16 ± 0.04	141.34 ± 23.01	153.19 ± 20.26
	Total	0.92 ± 0.02	456 ± 41	28.1 ± 3.9	0.31 ± 0.15	2.75 ± 4.44	3.06 ± 4.59	0.16 ± 0.04	141.34 ± 23.01	153.19 ± 20.26
Textile	Flaming	0.97 ± 0.01	1540 ± 129	27.3 ± 8.9	9.53 ± 1.95	1.17 ± 0.19	10.70 ± 5.58	4.43 ± 2.12	37.20 ± 22.65	42.78 ± 31.32
	Smoldering	0.86 ± 0.03	1227 ± 59	149.5 ± 34.5	11.57 ± 8.73	1.19 ± 0.53	12.76 ± 9.87	1.68 ± 0.45	75.56 ± 15.33	87.55 ± 24.71
	Total	0.87 ± 0.03	1467 ± 104	54.9 ± 7.4	10.37 ± 3.72	1.21 ± 0.15	11.58 ± 6.57	3.72 ± 1.48	47.04 ± 16.83	53.95 ± 26.96
Plastic Bottles	Flaming		No Flaming Phase							
	Smoldering	0.56 ± 0.05	182 ± 42	90.4 ± 10.6	0.22 ± 0.26	0.12 ± 0.08	0.35 ± 0.34	0.22 ± 0.02	651.00 ± 38.45	722.47 ± 17.98
	Total	0.56 ± 0.05	182 ± 42	90.4 ± 10.6	0.22 ± 0.26	0.12 ± 0.08	0.35 ± 0.34	0.22 ± 0.02	651.00 ± 38.45	722.47 ± 17.98
Plastic Bags	Flaming	0.98 ± 0.00	2938 ± 26	21.0 ± 5.1	0.70 ± 0.17	0.72 ± 0.04	1.42 ± 0.14	0.08 ± 0.01	33.48 ± 9.22	36.01 ± 9.62
	Smoldering	0.89 ± 0.01	2506 ± 247	183.9 ± 13.7	3.74 ± 0.82	6.87 ± 2.62	10.61 ± 3.15	0.36 ± 0.17	85.75 ± 76.56	89.47 ± 76.47
	Total	0.94 ± 0.01	2934 ± 24	22.4 ± 5.4	0.72 ± 0.17	0.77 ± 0.06	1.50 ± 0.12	0.08 ± 0.01	34.00 ± 8.55	36.55 ± 8.88
Vegetation (0% mc[a])	Flaming	0.97 ± 0.01	1573 ± 11	21.0 ± 3.6	2.94 ± 0.42	0.40 ± 0.15	3.34 ± 0.21	0.72 ± 0.14	3.80 ± 1.07	3.60 ± 0.83
	Smoldering	0.84 ± 0.02	1366 ± 18	156.2 ± 13.6	1.87 ± 0.16	0.29 ± 0.03	2.17 ± 0.12	0.12 ± 0.02	1.70 ± 1.68	1.57 ± 1.48
	Total	0.88 ± 0.01	1515 ± 12	58.5 ± 4.8	2.64 ± 0.32	0.37 ± 0.12	3.01 ± 0.11	0.54 ± 0.08	3.20 ± 1.25	3.02 ± 1.01
Vegetation (20% mc[a])	Flaming	0.93 ± 0.04	1549 ± 14	34.7 ± 8.1	2.42 ± 0.13	0.74 ± 0.12	3.16 ± 0.24	0.76 ± 0.10	5.40 ± 1.00	5.56 ± 1.14
	Smoldering	0.87 ± 0.02	1390 ± 7	135.5 ± 15.2	1.43 ± 0.08	0.47 ± 0.09	1.90 ± 0.01	0.20 ± 0.08	5.88 ± 7.27	6.18 ± 7.68
	Total	0.91 ± 0.03	1505 ± 1	63.9 ± 3.3	2.17 ± 0.07	0.64 ± 0.07	2.82 ± 0.13	0.56 ± 0.07	4.80 ± 1.98	4.97 ± 2.16
Vegetation (50% mc[a])	Flaming		No Flaming Phase							
	Smoldering	0.79 ± 0.00	1124 ± 0	183.6 ± 0.7	1.64 ± 0.15	0.25 ± 0.04	1.88 ± 0.19	0.28 ± 0.05	87.57 ± 6.83	92.66 ± 7.24
	Total	0.79 ± 0.00	1124 ± 0	183.6 ± 0.7	1.64 ± 0.15	0.25 ± 0.04	1.88 ± 0.19	0.28 ± 0.05	87.57 ± 6.83	92.66 ± 7.24
Food	Flaming		No Flaming Phase							
	Smoldering	0.89 ± 0.01	955 ± 30	76.1 ± 7.6	1.71 ± 0.34	0.27 ± 0.01	1.98 ± 0.34	0.16 ± 0.02	82.97 ± 18.36	87.23 ± 20.76
	Total	0.89 ± 0.01	955 ± 30	76.1 ± 7.6	1.71 ± 0.34	0.27 ± 0.01	1.98 ± 0.34	0.16 ± 0.02	82.97 ± 18.36	87.23 ± 20.76
Combined	Flaming	0.98 ± 0.00	1443 ± 8	14.9 ± 0.7	1.66 ± 0.14	0.63 ± 0.03	2.29 ± 0.16	1.13 ± 0.15	6.94 ± 2.32	7.34 ± 2.36
	Smoldering	0.88 ± 0.02	1302 ± 28	105.1 ± 11.0	2.40 ± 0.19	0.55 ± 0.09	2.95 ± 0.26	0.17 ± 0.06	6.55 ± 3.01	6.95 ± 3.22
	Total	0.91 ± 0.01	1417 ± 8	31.6 ± 1.8	1.80 ± 0.11	0.61 ± 0.00	2.41 ± 0.11	0.95 ± 0.13	6.86 ± 2.08	7.26 ± 2.12

[a]mc: fuel moisture content

Table 3: Comparison of emission factors from this study with those reported in the literature.

Ref.	Region	Fuel	Emission Factor (g kg^{-1} fuel)						Method
			CO_2	CO	NO_x (as NO_2)	SO_2	$PM_{2.5}$	PM_{10}	
Paper									
This study	**South Africa**	**Paper**	**1498 ± 7**	**44.9 ± 3.2**	**1.14 ± 0.31**	**0.57 ± 0.41**	**13.31 ± 0.77**	**13.42 ± 1.21**	**Lab**
(Park et al., 2013)	South Korea	Paper					0.6 (0.25–0.8)	0.93 (0.73–1.13)	Lab
(Thai et al., 2016; Xiu et al., 2018)	Marshall Islands	Paper briquettes		112	5.7		2.0		Lab
Leather/Rubber/Tires									
This study	**South Africa**	**Car floor mat**	**456 ± 41**	**28.1 ± 3.9**	**3.06 ± 4.59**	**0.16 ± 0.04**	**141.34 ± 23.01**	**153.19 ± 20.26**	**Lab**
(Ryan, 1989)	USA	Chunk tire						108–119	Lab
(Ryan, 1989)	USA	Shredded tire						119–179	Lab
(Downard et al., 2015)	USA	Shredded tires				7.1±8.3	5.35±5.39		Field
(Stockwell, 2016)	USA	Shredded tire	2882±14	70.6±6.4	7.81	26.2±2.2			Lab
Textile/fabric									
This study	**South Africa**	**Mixed fabrics**	**1467 ± 104**	**54.9 ± 7.4**	**11.58 ± 6.57**	**3.72 ± 1.48**	**47.04 ± 16.83**	**53.95 ± 26.96**	**Lab**
(Wesolek and Kozlowski, 2002)	Poland	Natural fabrics	850–1300	50–215	0.15–0.43	0.1–1.1			Lab
(Wesolek and Kozlowski, 2002)	Poland	Synthetic fabrics	1000–1750	21–139	0.1–0.33	0.06–0.07			
Plastics									
This study	**South Africa**	**Plastic bottles**	**182 ± 42**	**90.4 ± 10.6**	**0.35 ± 0.34**	**0.22 ± 0.02**	**651.00 ± 38.45**	**722.47 ± 17.98**	**Lab**
This study	**South Africa**	**Plastic bags**	**2934 ± 24**	**22.4 ± 5.4**	**1.50 ± 0.12**	**0.08 ± 0.01**	**34.00 ± 8.55**	**36.55 ± 8.88**	**Lab**
(Park et al., 2013)	South Korea	Plastics					0.5 (0.1–0.85)	1.5 (0.6–2.4)	Lab
(Lemieux et al., 2004; Oberacker et al., 1992)	USA	Agricultural plastic film						5.7	Lab

Ref.	Region	Fuel	Emission Factor (g kg^{-1} fuel)						Method
			CO_2	CO	NO_x (as NO_2)	SO_2	$PM_{2.5}$	PM_{10}	
(Stockwell et al., 2016; Jayarathne et al., 2018)	Nepal	Chip bags	2249	15.9	4.30	bdl[a]	50±9		Field
(Stockwell et al., 2016; Jayarathne et al., 2018)	Nepal	Plastics	2473–2695	16.6–62.2	5.31	bdl[a]	84±13		Field
(Stockwell, 2016)	USA	Plastic bag	3127	11.7	2.69				Lab
Vegetation									
This study	**South Africa**	**Vegetation (0% mc[a])**	**1515 ± 12**	**58.5 ± 4.8**	**3.01 ± 0.11**	**0.54 ± 0.08**	**3.20 ± 1.25**	**3.02 ± 1.01**	**Lab**
This study	**South Africa**	**Vegetation (20% mc[a])**	**1505 ± 1**	**63.9 ± 3.3**	**2.82 ± 0.13**	**0.56 ± 0.07**	**4.80 ± 1.98**	**4.97 ± 2.16**	**Lab**
This study	**South Africa**	**Vegetation (50% mc[a])**	**1124 ± 0**	**183.6 ± 0.7**	**1.88 ± 0.19**	**0.28 ± 0.05**	**87.57 ± 6.83**	**92.66 ± 7.24**	**Lab**
(Christian et al., 2010)	Mexico	Barley stubble	1602	118					Field
(Akagi et al., 2011)	Africa	Savanna vegetation	1686±38	63±17	6.0±1.2	0.48±0.27	7.17±3.42		Data synthesis
(Akagi et al., 2011)	Global	Crop residue	1585±100	102±33	4.8±2.4		6.26±2.36		
(Santiago-De La Rosa et al., 2018)	Mexico	Alfalfa	1052±144	65.23±5.38			9.98 ± 0.71	11.11±0.91	Lab
(Santiago-De La Rosa et al., 2018)	Mexico	Barley	1693±84	33.31±2.33			1.19 ± 0.10	1.77±0.19	Lab
(Santiago-De La Rosa et al., 2018)	Mexico	Bean	1230±38	65.92±3.5			2.24 ± 0.19	2.75±0.18	Lab
(Santiago-De La Rosa et al., 2018)	Mexico	Cotton	1690±76	75.81±4.1			8.22 ± 0.54	13.37±1.9	Lab
(Santiago-De La Rosa et al., 2018)	Mexico	Maize	1748±81	34.61±2.04			2.70 ± 0.28	3.3±0.42	Lab
(Santiago-De La Rosa et al., 2018)	Mexico	Rice	1651±54	81.12±3.25			3.04 ± 0.24	4.95±0.52	Lab
(Santiago-De La Rosa et al., 2018)	Mexico	Sorghum	1851±58	155.71±4.77			11.30 ± 1.05	21.56±2.26	Lab
(Santiago-De La Rosa et al., 2018)	Mexico	Wheat	1812±103	28.85±1.79			2.54 ± 0.39	4.07±0.51	Lab
(Yokelson et al., 2009)	Mexico	Crop residues	1676±50	75.04±26.81	7.21±2.69				Field
(Yokelson et al., 2009)	Mexico	Deforestation	1656±38	82.68±14.21	7.20±2.72				Field

Ref.	Region	Fuel	Emission Factor (g kg^{-1} fuel)						Method
			CO_2	CO	NO_x (as NO_2)	SO_2	$PM_{2.5}$	PM_{10}	
(Ni et al., 2015)	China	Wheat straw	1311±181	47.9±13.5			11.4±4.9		Lab
(Ni et al., 2015)	China	Rice straw	1393±91	57.2±26.0			8.5±6.7		Lab
(Ni et al., 2015)	China	Corn stalk	1363±154	52.1±17.7			12.0±5.4		Lab
Mixed household/municipal waste									
This study	**South Africa**	**Combined waste**	**1417 ± 8**	**31.6 ± 1.8**	**2.41 ± 0.11**	**0.95 ± 0.13**	**6.86 ± 2.08**	**7.26 ± 2.12**	**Lab**
(U.S. Epa, 1992; Gerstle and Kemnitz, 1967)	USA	Municipal refuse	615	42	3	0.5		8 (TSP) [c]	Lab
(Lemieux, 1997, 1998)	USA	Household waste (no recycle)					14.8–20.07	16.23–21.28	Lab
(Lemieux, 1997, 1998)	USA	Household waste (recycle)					3.58–6.93	4.18–7.46	Lab
(Christian et al., 2010)	Mexico	Landfill garbage	1367±65	45.3±22.8			10.5±8.8		Field
(Park et al., 2013)	South Korea	Household solid waste					0.78 (0.48–0.98)	1.2 (0.3–1.9)	Lab
(Stockwell et al., 2016; Jayarathne et al., 2018)	Nepal	Mixed garbage	1602±142	84.7±55.5	3.39±0.21	bdl [b]	7.37±1.22		Field
(Jayarathne et al., 2018)	Nepal	Damp mixed garbage					124±23 82±13		Field
(Akagi et al., 2011; Reyna-Bensusan et al., 2018; Wiedinmyer et al., 2014)	Global	Mixed garbage	1453±69	38±19	5.7±2.3	0.5	9.8±5.7	11.9	Data synthesis
(Yokelson et al., 2013)	USA	Mixed garbage	1341	28.7	1.35	0.77	10.8		Lab
(Stockwell, 2016)	USA	Mixed household refuse	1793±28	31.5±6.9	1.57±0.41	0.897			Lab

Ref.	Region	Fuel	Emission Factor (g kg^{-1} fuel)						Method
			CO_2	CO	NO_x (as NO_2)	SO_2	$PM_{2.5}$	PM_{10}	
Paper									
This study	**South Africa**	**Paper**	**1498 ± 7**	**44.9 ± 3.2**	**1.14 ± 0.31**	**0.57 ± 0.41**	**13.31 ± 0.77**	**13.42 ± 1.21**	**Lab**
(Park et al., 2013)	South Korea	Paper					0.6 (0.25–0.8)	0.93 (0.73–1.13)	Lab
(Thai et al., 2016; Xiu et al., 2018)	Marshall Islands	Paper briquettes		112	5.7		2.0		Lab
(Cheng et al., 2020)	China	Paper	1400±100	66.6±11.5	3.3±0.3	0.30±0.07	10.56±1.52		Barrel
(Cheng et al., 2020)	China	Paper	1000±100	34.1±6.7	2.3±0.2	0.20±0.08	5.81±0.39		Pile
(Wu et al., 2021)	China	Paper packaging					4.90±1.12		Field
Leather/Rubber/Tires									
This study	**South Africa**	**Car floor mat**	**456 ± 41**	**28.1 ± 3.9**	**3.06 ± 4.59**	**0.16 ± 0.04**	**141.34 ± 23.01**	**153.19 ± 20.26**	**Lab**
(Ryan, 1989)	USA	Chunk tire						108–119	Lab
(Ryan, 1989)	USA	Shredded tire						119–179	Lab
(Downard et al., 2015)	USA	Shredded tires				7.1±8.3	5.35±5.39		Field
(Stockwell, 2016)	USA	Shredded tire	2882±14	70.6±6.4	7.81	26.2±2.2			Lab
Textile/fabric									
This study	**South Africa**	**Mixed fabrics**	**1467 ± 104**	**54.9 ± 7.4**	**11.58 ± 6.57**	**3.72 ± 1.48**	**47.04 ± 16.83**	**53.95 ± 26.96**	**Lab**
(Wesolek and Kozlowski, 2002)	Poland	Natural fabrics	850–1300	50–215	0.15–0.43	0.1–1.1			Lab
(Wesolek and Kozlowski, 2002)	Poland	Synthetic fabrics	1000–1750	21–139	0.1–0.33	0.06–0.07			
(Cheng et al., 2020)	China	Textile	1200±98	37.5±7.4	2.1±0.1	0.10±0.03	9.27±0.61		Barrel
(Cheng et al., 2020)	China	Textile	800±68	19.6±3.0	0.6±0.1	0.10±0.02	5.56±0.42		Pile
Plastics									
This study	**South Africa**	**Plastic bottles**	**182 ± 42**	**90.4 ± 10.6**	**0.35 ± 0.34**	**0.22 ± 0.02**	**651.00 ± 38.45**	**722.47 ± 17.98**	**Lab**
This study	**South Africa**	**Plastic bags**	**2934 ± 24**	**22.4 ± 5.4**	**1.50 ± 0.12**	**0.08 ± 0.01**	**34.00 ± 8.55**	**36.55 ± 8.88**	**Lab**

Ref.	Region	Fuel	Emission Factor (g kg^{-1} fuel)						Method
			CO_2	CO	NO_x (as NO_2)	SO_2	$PM_{2.5}$	PM_{10}	
(Park et al., 2013)	South Korea	Plastics					0.5 (0.1–0.85)	1.5 (0.6–2.4)	Lab
(Lemieux et al., 2004; Oberacker et al., 1992)	USA	Agricultural plastic film						5.7	Lab
(Stockwell et al., 2016; Jayarathne et al., 2018)	Nepal	Chip bags	2249	15.9	4.30	bdl[a]	50±9		Field
(Stockwell et al., 2016; Jayarathne et al., 2018)	Nepal	Plastics	2473–2695	16.6–62.2	5.31	bdl[a]	84±13		Field
(Stockwell, 2016)	USA	Plastic bag	3127	11.7	2.69				Lab
(Wu et al., 2021)	China	Plastic woven bags					2.60±0.46		Field
(Wu et al., 2021)	China	Plastic packaging					2.61±0.45		Field
(Wu et al., 2021)	China	Plastic foam					34.8±4.5		Field
Vegetation									
This study	**South Africa**	**Vegetation (0% mc[a])**	**1515 ± 12**	**58.5 ± 4.8**	**3.01 ± 0.11**	**0.54 ± 0.08**	**3.20 ± 1.25**	**3.02 ± 1.01**	**Lab**
This study	**South Africa**	**Vegetation (20% mc[a])**	**1505 ± 1**	**63.9 ± 3.3**	**2.82 ± 0.13**	**0.56 ± 0.07**	**4.80 ± 1.98**	**4.97 ± 2.16**	**Lab**
This study	**South Africa**	**Vegetation (50% mc[a])**	**1124 ± 0**	**183.6 ± 0.7**	**1.88 ± 0.19**	**0.28 ± 0.05**	**87.57 ± 6.83**	**92.66 ± 7.24**	**Lab**
(Christian et al., 2010)	Mexico	Barley stubble	1602	118					Field
(Akagi et al., 2011)	Africa	Savanna vegetation	1686±38	63±17	6.0±1.2	0.48±0.27	7.17±3.42		Data synthesis
(Akagi et al., 2011)	Global	Crop residue	1585±100	102±33	4.8±2.4		6.26±2.36		
(Santiago-De La Rosa et al., 2018)	Mexico	Alfalfa	1052±144	65.23±5.38			9.98 ± 0.71	11.11±0.91	Lab
(Santiago-De La Rosa et al., 2018)	Mexico	Barley	1693±84	33.31±2.33			1.19 ± 0.10	1.77±0.19	Lab
(Santiago-De La Rosa et al., 2018)	Mexico	Bean	1230±38	65.92±3.5			2.24 ± 0.19	2.75±0.18	Lab
(Santiago-De La Rosa et al., 2018)	Mexico	Cotton	1690±76	75.81±4.1			8.22 ± 0.54	13.37±1.9	Lab
(Santiago-De La Rosa et al., 2018)	Mexico	Maize	1748±81	34.61±2.04			2.70 ± 0.28	3.3±0.42	Lab
(Santiago-De La Rosa et al., 2018)	Mexico	Rice	1651±54	81.12±3.25			3.04 ± 0.24	4.95±0.52	Lab
(Santiago-De La Rosa et al., 2018)	Mexico	Sorghum	1851±58	155.71±4.77			11.30 ± 1.05	21.56±2.26	Lab

Ref.	Region	Fuel	Emission Factor (g kg^{-1} fuel)						Method
			CO_2	CO	NO_x (as NO_2)	SO_2	$PM_{2.5}$	PM_{10}	
(Santiago-De La Rosa et al., 2018)	Mexico	Wheat	1812±103	28.85±1.79			2.54 ± 0.39	4.07±0.51	Lab
(Yokelson et al., 2009)	Mexico	Crop residues	1676±50	75.04±25.81	7.21±2.69				Field
(Yokelson et al., 2009)	Mexico	Deforestation	1656±38	82.68±14.21	7.20±2.72				Field
(Ni et al., 2015)	China	Wheat straw	1311±181	47.9±13.5			11.4±4.9		Lab
(Ni et al., 2015)	China	Rice straw	1393±91	57.2±26.0			8.5±6.7		Lab
(Ni et al., 2015)	China	Corn stalk	1363±154	52.1±17.7			12.0±5.4		Lab
(EMEP/EEA, 2019)	USA	Agricultural waste		55.83	3.18	0.11	4.19	4.51	Lab
Mixed household/municipal waste									
This study	**South Africa**	**Combined waste**	**1417 ± 8**	**31.6 ± 1.8**	**2.41 ± 0.11**	**0.95 ± 0.13**	**6.86 ± 2.08**	**7.26 ± 2.12**	**Lab**
(U.S. EPA, 1992; Gerstle and Kemnitz, 1967)	USA	Municipal refuse	615	42	3	0.5		8 (TSP) [c]	Lab
(Lemieux, 1997, 1998)	USA	Household waste (no recycle)					14.8–20.07	16.23–21.28	Barrel
(Lemieux, 1997, 1998)	USA	Household waste (recycle)					3.58–6.93	4.18–7.46	Barrel
(Christian et al., 2010)	Mexico	Landfill garbage	1367±65	45.3±22.8			10.5±8.8		Field
(Park et al., 2013)	South Korea	Household solid waste					0.78 (0.48–0.98)	1.2 (0.3–1.9)	Lab
(Stockwell et al., 2016; Jayarathne et al., 2018)	Nepal	Mixed garbage	1602±142	84.7±55.5	3.39±0.21	bdl[b]	7.37±1.22		Field
(Jayarathne et al., 2018)	Nepal	Damp mixed garbage					124±23 82±13		Field
(Akagi et al., 2011; Reyna-Bensusan et al., 2018; Wiedinmyer et al., 2014)	Global	Mixed garbage	1453±69	38±19	5.7±2.3	0.5	9.8±5.7	11.9	Data synthesis
(Yokelson et al., 2013)	USA	Mixed garbage	1341	28.7	1.35	0.77	10.8		Lab
(Stockwell, 2016)	USA	Mixed household refuse	1793±28	31.5±6.9	1.57±0.41	0.897			Lab
(Cheng et al., 2020)	China	Mixed waste	1230±95	55.1±10.5	2.4±0.3	0.50±0.08	10.53±1.24		Barrel
(Cheng et al., 2020)	China	Mixed waste	1000±70	25.9±4.9	1.2±0.1	0.20±0.05	6.04±0.91		Pile

[a]mc: moisture content

[b]bdl: below detection limit
[c]TSP: total suspended particulate

3.4 Effects of Ash and Particulate Carbon Content on EF Calculation

Carbon contents in the ash or PM emissions (Eq. (2)) are rarely included in fuel-based EF calculations (Stockwell et al., 2016; Christian et al., 2010; Jayarathne et al., 2018; Wang et al., 2019; Chen et al., 2007). Their impacts are assumed to be negligible but have not been systematically evaluated. Table 4~~Table 4~~ demonstrates the importance of carbon in ash $\left(\frac{m_{ash}}{m_{fuel}} CMF_{ash}/CMF_{fuel}\right)$ and ~~in~~ PM $\left(C_{PM}/\left[C_{CO_2}\left(\frac{M_c}{M_{CO_2}}\right) + C_{CO}\left(\frac{M_c}{M_{CO}}\right) + C_{PM}\right]\right)$ in EF calculations using Eq. (2). Without including ash and/or PM carbon, changes in EFs are <5% for flaming dominated combustion of paper, plastic bags, vegetation with 0% and 20% moisture content, and combined materials. These fuels had <5% fuel carbon in ash and <5% emitted carbon in PM.

Table 4: Emission factor changes relative to Eq. (2) when the carbon in the PM (C_{PM}) or ash (CMF_{ash}) are not included.

Fuel	Fuel Carbon in Ash	Emitted Carbon in PM_{10}	EF Changes relative to Eq. (2)		
			With Ash Without C_{PM}	Without Ash With C_{PM}	Without Ash Without C_{PM}
Paper	1.1 ± 0.3%	1.9 ± 0.3%	1.9%	1.1%	3.1%
Rubber	22.6 ± 1.0%	46.5 ± 4.5%	87.0%	29.1%	141.4%
Textile	2.1 ± 0.4%	9.4 ± 6.6%	10.4%	2.2%	12.8%
Plastic Bottle	6.4 ± 3.8%	85.2 ± 1.9%	576.6%	6.9%	623.1%
Plastic Bag	0.4 ± 0.1%	3.7 ± 0.6%	3.8%	0.4%	4.3%
Vegetation (0% mc[a])	1.2 ± 0.4%	0.5 ± 0.1%	0.5%	1.2%	1.7%
Vegetation (20% mc[a])	1.2 ± 0.2%	0.7 ± 0.3%	0.7%	1.2%	1.9%
Vegetation (50% mc*)	1.0 ± 0.2%	12.7 ± 0.1%	14.5%	1.1%	15.7%
Food	2.5 ± 0.6%	13.6 ± 2.8%	15.7%	2.5%	18.7%
Combined	1.1 ± 0.5%	1.5 ± 0.5%	1.5%	1.2%	2.7%

[a]mc: fuel moisture content

The consequences of not including ash or PM carbon are larger for smoldering fuels. Due to their high EFs of carbonaceous PM, the errors caused by not including PM carbon are over 10%. Rubber had the highest fuel carbon (22.6%) in the ash, and excluding ash in Eq. (2) results in a 29.1% overestimation of EFs. Rubber had 46.5% carbon emitted as TC in PM; excluding C_{PM} causes an EF overestimation of 87%. If neither ash nor PM carbon is included, the EFs are overestimated by 141%. The hard plastic bottle EFs are also affected by carbon contents. Because of the very high EFs for carbonaceous PM and relatively low EFs for CO and CO_2, 85% of the carbon was emitted as PM. Not including C_{PM} results in an EF overestimation of 577%; in addition, if ash carbon is not included, the EFs are overestimated by 623%.

This result shows that ash and PM carbon cannot be neglected in EF calculations, particularly for smoldering combustion with high carbon contents in ash and/or PM emissions. Carbon can also be emitted as gaseous hydrocarbons and excluding it in Eq. (2) may result in some overestimation of the EFs. While it is expected that the hydrocarbon carbon content is lower than that in CO and CO_2 in most cases, it may not be negligible when their emissions are high. Future studies should measure total hydrocarbons for more accurate EF determination.

3.5 Discussion: Emission Factors for Solid Waste Open Burning Emission Inventories

One application of EFs is to estimate emission rates for establishing ~~relevant regions in~~ emission inventories (U.S. EPA, 1992). These inventories are used to conduct air quality modeling, track long-term trends, evaluate control strategy effectiveness, and provide offsets for other emitters. For example, emissions avoided by trucking the normally open burned household solid waste to landfill by Sasol's WCI can be estimated as:

$$E_p = AR \times EF_p = \sum_{i=1}^{n} AR_i \times EF_{p,i} \quad (3)$$

where E_p is total avoided emission of pollutant p (in metric tons per year); AR is the activity rate, i.e., the amount of burned waste avoided in a year (in tons per year); and EF_p is the emission factor (in grams of emissions per gram of waste) of pollutant p from the waste that would otherwise be burned. The subscript i corresponds to values for each waste material ~~i~~ (e.g., paper, textile, plastics, and vegetation). EF_p corresponds to the measured EFs from the combined waste materials; it can also be estimated by summing $EF_{p,i}$ for individual waste materials, weighted by their mass fractions (Fig. 1). $EF_{p,i}$ can be determined from laboratory testing under controlled conditions, and the heterogeneity of waste materials can be accounted for by examining the waste refuse. The separation of flaming and smoldering EFs offers additional flexibility in accounting for burning condition changes. However, it should be cautioned that the burning behaviors differ between separated and combined waste materials, causing emissions to change. Table S5~~Table S5~~ compares the measured EFs for the combined materials and the values calculated from $EF_{p,i}$. The calculated EFs agree with the measured values within 10% for CO_2 and NO_x; however, the calculated EFs for CO and PM are over 50% and 600% higher, respectively. It is possible that more efficient combustion in the combined materials lowered CO and PM emissions as compared to less efficient individual burns, particularly for materials that only smoldered and had high EFs for CO and PM. Additionally, laboratory measured $EF_{p,i}$ or EF_p might differ from field values given the complex waste mixtures and burning conditions. Adjustments to laboratory $EF_{p,i}$ might be needed when estimating real-world EF_p. Future studies comparing in situ measurement from a variety of representative real-world burns with laboratory data would assist in establishing adjustment factors.

4 Conclusions

This study measured criteria pollutant emissions from simulated combustion of different household solid waste materials representative of those in open burnings in South Africa. EFs vary with waste composition and combustion conditions. Data from this study fill EF gaps for paper, leather/rubber, textile, and food discards burning that have been scarcely reported in the literature. EFs for vegetation and mixed waste materials from this study are within the ranges reported in the literature. These EFs can be used to improve emission inventories for household and municipal solid waste open burning emissions in South Africa and other countries.

Emissions are closely related fuel elemental compositions. Among the tested materials, plastic bags have the highest carbon content and the highest combustion efficiency, leading to the highest EFs for CO_2. Textiles have the highest abundances

of nitrogen and sulfur, resulting in the highest EFs for NO_x and SO_2. Combustion behaviors and emissions are also affected by fuel moisture content. EFs for vegetation with three moisture content: dry (0%), natural (20%), and damp (50%) were measured. Emissions were similar for 0% and 20% moisture content; however, EFs for CO and PM from the vegetation with 50% moisture content are 3 and 20–30 times, respectively, ~~of~~ those from 0% and 20% moisture content.

This study reports three sets of EF_s (i.e., flaming, smoldering, and entire combustion), which can be applied to estimate emissions based on waste burning characteristics. It also reports EFs for individual and combined waste categories. These data offer flexibility in calculating emission rates depending on waste composition and burning characteristics. However, caution should be exerted when using mass weighted sum of individual waste category EFs to calculate combined waste EFs as the combustion behavior might be different between individual and combined waste materials. This study shows that neglecting the carbon in ash and/or PM may lead to significant overestimation of EFs.

EF data from this study were obtained from controlled laboratory tests simulating real-world open burning conditions. Real-world open burning emissions vary with waste material composition, pile size, packing structure, moisture content, ambient temperature, and wind speed. Such variations are reflected in the wide range of EFs reported in the literature. Although this and past studies agree within reported extremes, laboratory tests are an approximation of real-world variations. The EFs derived from laboratory experiments represent the values obtained under the specific conditions in laboratory tests; adjustment might be needed when real-world burning conditions are very different from laboratory test conditions.

Data availability. Data is available upon request.

Author contributions. XW, JCC, and JGW designed the study; HF conducted the combustion experiments; XW and HF performed the data analyses and prepared the original paper draft; WC and SDV provided waste materials and resources; all authors reviewed and edited the paper.

Competing interests. None.

Financial support. This research was partially funded by SASOL and partially by the Desert Research Institute internal funding.

Acknowledgements: The authors thank Matthew Claassen of DRI for collecting vegetations for testing.

References

Akagi, S. K., Yokelson, R. J., Wiedinmyer, C., Alvarado, M. J., Reid, J. S., Karl, T., Crounse, J. D., and Wennberg, P. O.: Emission factors for open and domestic biomass burning for use in atmospheric models, Atmos. Chem. Phys., 11, 4039-4072, 10.5194/acp-11-4039-2011, 2011.

Andreae, M. O. and Gelencsér, A.: Black carbon or brown carbon? The nature of light-absorbing carbonaceous aerosols, Atmos. Chem. Phys., 6, 3131-3148, 2006.
Bond, T. C., Streets, D. G., Yarber, K. F., Nelson, S. M., Woo, J.-H., and Klimont, Z.: A technology-based global inventory of black and organic carbon emissions from combustion, J. Geophys. Res., 109, D14203, 10.1029/2003jd003697, 2004.
Bond, T. C., Doherty, S. J., Fahey, D. W., Forster, P. M., Berntsen, T., DeAngelo, B. J., Flanner, M. G., Ghan, S., Kärcher, B., and Koch, D.: Bounding the role of black carbon in the climate system: A scientific assessment, Journal of geophysical research: Atmospheres, 118, 5380-5552, 2013.
Chen, L.-W. A., Chow, J. C., Wang, X., Cao, J., Mao, J., and Watson, J. G.: Brownness of Organic Aerosol over the United States: Evidence for Seasonal Biomass Burning and Photobleaching Effects, Environ. Sci. Technol., 55, 8561-8572, 10.1021/acs.est.0c08706, 2021.
Chen, L.-W. A., Verburg, P., Shackelford, A., Zhu, D., Susfalk, R., Chow, J. C., and Watson, J. G.: Moisture effects on carbon and nitrogen emission from burning of wildland biomass, Atmos. Chem. Phys., 10, 6617-6625, doi:10.5194/acp-10-6617-2010, 2010.
Chen, L.-W. A., Chow, J. C., Wang, X. L., Robles, J. A., Sumlin, B., Lowenthal, D. H., Zimmermann, R., and Watson, J. G.: Multi-wavelength optical measurement to enhance thermal/optical analysis for carbonaceous aerosol, Atmos. Meas. Tech., 8, 451-461, doi:10.5194/amt-8-451-2015, 2015.
Chen, L.-W. A., Moosmüller, H., Arnott, W. P., Chow, J. C., Watson, J. G., Susott, R. A., Babbitt, R. E., Wold, C. E., Lincoln, E. N., and Hao, W. M.: Emissions from Laboratory Combustion of Wildland Fuels: Emission Factors and Source Profiles, Environ. Sci. Technol., 41, 4317-4325, 10.1021/es062364i, 2007.
Cheng, K., Hao, W., Wang, Y., Yi, P., Zhang, J., and Ji, W.: Understanding the emission pattern and source contribution of hazardous air pollutants from open burning of municipal solid waste in China, Environ. Pollut., 263, 114417, https://doi.org/10.1016/j.envpol.2020.114417, 2020.
Chow, J. C., Watson, J. G., Chen, L.-W. A., Chang, M. C. O., Robinson, N. F., Trimble, D., and Kohl, S.: The IMPROVE_A temperature protocol for thermal/optical carbon analysis: maintaining consistency with a long-term database, Journal of the Air & Waste Management Association, 57, 1014-1023, 2007.
Chow, J. C., Cao, J. J., Chen, L.-W. A., Wang, X. L., Wang, Q. Y., Tian, J., Ho, S. S. H., Watts, A. C., Carlson, T. N., Kohl, S. D., and Watson, J. G.: Changes in $PM_{2.5}$ peat combustion source profiles with atmospheric aging in an oxidation flow reactor, Atmos. Meas. Tech., 12, 5475-5501, https://doi.org/10.5194/amt-2019-198, 2019.
Christian, T. J., Yokelson, R. J., Cárdenas, B., Molina, L. T., Engling, G., and Hsu, S. C.: Trace gas and particle emissions from domestic and industrial biofuel use and garbage burning in central Mexico, Atmos. Chem. Phys., 10, 565-584, 10.5194/acp-10-565-2010, 2010.
Cook, E. and Velis, C.: Global review on safer end of engineered life, Royal Academy of Engineering, London, UK, https://doi.org/10.5518/100/58, 2021.
Cronjé, N., Van der Merwe, I., and Müller, I.-M.: Household food waste: A case study in Kimberley, South Africa, Journal of Consumer Sciences, 46, 2018.
Downard, J., Singh, A., Bullard, R., Jayarathne, T., Rathnayake, C. M., Simmons, D. L., Wels, B. R., Spak, S. N., Peters, T., Beardsley, D., Stanier, C. O., and Stone, E. A.: Uncontrolled combustion of shredded tires in a landfill – Part 1: Characterization of gaseous and particulate emissions, Atmos. Environ., 104, 195-204, https://doi.org/10.1016/j.atmosenv.2014.12.059, 2015.
EMEP/EEA: EMEP/EEA air pollutant emission inventory guidebook 2019, European Environmental Agency, Copenhagen, Denmark, 2019.
Ferronato, N. and Torretta, V.: Waste Mismanagement in Developing Countries: A Review of Global Issues, Int J Environ Res Public Health, 16, 10.3390/ijerph16061060, 2019.
Gerstle, R. W. and Kemnitz, D. A.: Atmospheric Emissions from Open Burning, Journal of the Air Pollution Control Association, 17, 324-327, 10.1080/00022470.1967.10468988, 1967.
Holland, B. J. and Hay, J. N.: The thermal degradation of PET and analogous polyesters measured by thermal analysis–Fourier transform infrared spectroscopy, Polymer, 43, 1835-1847, https://doi.org/10.1016/S0032-3861(01)00775-3, 2002.
IPCC: 2006 IPCC guidelines for national greenhouse gas inventories, National Greenhouse Gas Inventories Programme Japan; Intergovernmental Panel on Climate Change (IPCC): Geneva, Switzerland, 2006.

IPCC: Climate change 2013: The physical science basis. Working Group I Contribution to the Fifth Assessment Report of the Intergovernmental Panel on Climate Change, Cambridge University Press Cambridge, UK, and New York2013.

Jayarathne, T., Stockwell, C. E., Bhave, P. V., Praveen, P. S., Rathnayake, C. M., Islam, M. R., Panday, A. K., Adhikari, S., Maharjan, R., Goetz, J. D., DeCarlo, P. F., Saikawa, E., Yokelson, R. J., and Stone, E. A.: Nepal Ambient Monitoring and Source Testing Experiment (NAMaSTE): emissions of particulate matter from wood- and dung-fueled cooking fires, garbage and crop residue burning, brick kilns, and other sources, Atmos. Chem. Phys., 18, 2259-2286, 10.5194/acp-18-2259-2018, 2018.

Kodros, J. K., Wiedinmyer, C., Ford, B., Cucinotta, R., Gan, R., Magzamen, S., and Pierce, J. R.: Global burden of mortalities due to chronic exposure to ambient PM 2.5 from open combustion of domestic waste, Environ. Res. Lett., 11, 124022, 10.1088/1748-9326/11/12/124022, 2016.

Kwatala, N., Naidoo, M., Naidoo, S., and Garland, R. M.: Estimated emissions of domestic waste burning in South Africa, 2019 Conference of the National Association for Clean Air, Western Cape, October 3-4, 2019,

Lebreton, L. and Andrady, A.: Future scenarios of global plastic waste generation and disposal, Palgrave Communications, 5, 6, 10.1057/s41599-018-0212-7, 2019.

Lemieux, P. M.: Evaluation of emissions from the open burning of household waste in barrels - Volume 1. Technical Report, National Risk Management Research Laboratory, US Environmental Protection Agency, Cincinnati, OHEPA-600/R-97-134a, 1997.

Lemieux, P. M.: Evaluation of emissions from the open burning of household waste in barrels - Project Summary, National Risk Management Research Laboratory, US Environmental Protection Agency, Cincinnati, OH EPA/600/SR-97/134, 1998.

Lemieux, P. M., Lutes, C. C., and Santoianni, D. A.: Emissions of organic air toxics from open burning: a comprehensive review, Prog. Energy Combust. Sci., 30, 1-32, https://doi.org/10.1016/j.pecs.2003.08.001, 2004.

Moosmüller, H., Mazzoleni, C., Barber, P., Kuhns, H., Keislar, R., and Watson, J.: On-road measurement of automotive particle emissions by ultraviolet lidar and transmissometer: Instrument, Environ. Sci. Technol., 37, 4971-4978, 2003.

Ni, H., Han, Y., Cao, J., Chen, L.-W. A., Tian, J., Wang, X. L., Chow, J. C., Watson, J. G., Wang, Q., Wang, P., Li, H., and Huang, R.-J.: Emission characteristics of carbonaceous particles and trace gases from open burning of crop residues in China, Atmos. Environ., 123, Part B, 399-406, http://dx.doi.org/10.1016/j.atmosenv.2015.05.007, 2015.

Oberacker, D. A., Lin, P. C., Shaul, G. M., Ferguson, D. T., Engleman, V. S., Jackson, T. W., Chapman, J. S., Evans, J. D., Martrano, R. J., and Evey, L. L.: Characterization of Emissions Formed from Open Burning of Pesticide Bags, in: Pesticide Waste Management, ACS Symposium Series, 510, American Chemical Society, 78-94, doi:10.1021/bk-1992-0510.ch007 10.1021/bk-1992-0510.ch007, 1992.

Park, Y. K., Kim, W., and Jo, Y. M.: Release of Harmful Air Pollutants from Open Burning of Domestic Municipal Solid Wastes in a Metropolitan Area of Korea, Aerosol Air Qual. Res., 13, 1365-1372, 10.4209/aaqr.2012.10.0272, 2013.

Rabaji, O. P.: Waste dumping in Sharpeville (Emfuleni Municipality): an investigation of the characteristics and the potential impacts on air quality, M.S., Environmental Management, North-West University, Potchefstroom, South Africa, 2019.

Reid, J. S., Koppmann, R., Eck, T. F., and Eleuterio, D. P.: A review of biomass burning emissions part II: intensive physical properties of biomass burning particles, Atmos. Chem. Phys., 5, 799-825, 10.5194/acp-5-799-2005, 2005.

Rein, G., Cleaver, N., Ashton, C., Pironi, P., and Torero, J. L.: The severity of smouldering peat fires and damage to the forest soil, CATENA, 74, 304-309, https://doi.org/10.1016/j.catena.2008.05.008, 2008.

Reyna-Bensusan, N., Wilson, D. C., and Smith, S. R.: Uncontrolled burning of solid waste by households in Mexico is a significant contributor to climate change in the country, Environ. Res., 163, 280-288, https://doi.org/10.1016/j.envres.2018.01.042, 2018.

Ryan, J. V.: Characterization of emissions from the simulated open burning of scrap tires, Acurex Corp. , Research Triangle Park, NCEPA-600/2-89-054, 1989.

Santiago-De La Rosa, N., González-Cardoso, G., Figueroa-Lara, J. d. J., Gutiérrez-Arzaluz, M., Octaviano-Villasana, C., Ramírez-Hernández, I. F., and Mugica-Álvarez, V.: Emission factors of atmospheric and climatic pollutants from crop residues burning, J. Air Waste Manage. Assoc., 68, 849-865, 10.1080/10962247.2018.1459326, 2018.

Schmid, O., Chand, D., Karg, E., Guyon, P., Frank, G. P., Swietlicki, E., and Andreae, M. O.: Derivation of the density and refractive index of organic matter and elemental carbon from closure between physical and chemical aerosol properties, Environ Sci Technol, 43, 1166-1172, 10.1021/es800570p, 2009.

Sovová, K., Ferus, M., Matulková, I., Španěl, P., Dryahina, K., Dvořák, O., and Civiš, S.: A study of thermal decomposition and combustion products of disposable polyethylene terephthalate (PET) plastic using high resolution fourier transform infrared spectroscopy, selected ion flow tube mass spectrometry and gas chromatography mass spectrometry, Mol. Phys., 106, 1205-1214, 10.1080/00268970802077876, 2008.

Stockwell, C. E.: Advanced measurements of undersampled globally significant biomass burning sources, Chemistry, The University of Montana, Missoula, MT, 2016.

Stockwell, C. E., Christian, T. J., Goetz, J. D., Jayarathne, T., Bhave, P. V., Praveen, P. S., Adhikari, S., Maharjan, R., DeCarlo, P. F., Stone, E. A., Saikawa, E., Blake, D. R., Simpson, I. J., Yokelson, R. J., and Panday, A. K.: Nepal Ambient Monitoring and Source Testing Experiment (NAMaSTE): emissions of trace gases and light-absorbing carbon from wood and dung cooking fires, garbage and crop residue burning, brick kilns, and other sources, Atmos. Chem. Phys., 16, 11043-11081, 10.5194/acp-16-11043-2016, 2016.

Thai, P., Rahman, M. M., Pourkhesalian, A. M., and Stevanovic, S.: Comparative investigations of combustion emissions from paper briquettes, International Laboratory for Air Quality and Health (ILAQH) at Queensland University of Technology (QUT), 2016.

Tian, J., Chow, J. C., Cao, J., Han, Y., Ni, H., Chen, L.-W. A., Wang, X. L., Huang, R., Moosmüller, H., and Watson, J. G.: A Biomass Combustion Chamber: Design, Evaluation, and a Case Study of Wheat Straw Combustion Emission Tests, Aerosol Air Qual. Res., 15, 2104-2114, 2015.

U.S. EPA: Compilation of Air Pollutant Emissions Factors AP-42, Fifth Edition Section 2.5 Open Burning, U.S. Environmental Protection Agency, Research Triangle Park, NCEPA AP-42, 1992.

Velis, C. A. and Cook, E.: Mismanagement of Plastic Waste through Open Burning with Emphasis on the Global South: A Systematic Review of Risks to Occupational and Public Health, Environ. Sci. Technol., 55, 7186-7207, 10.1021/acs.est.0c08536, 2021.

Wang, Q., Wang, L., Li, X., Xin, J., Liu, Z., Sun, Y., Liu, J., Zhang, Y., Du, W., Jin, X., Zhang, T., Liu, S., Liu, Q., Chen, J., Cheng, M., and Wang, Y.: Emission characteristics of size distribution, chemical composition and light absorption of particles from field-scale crop residue burning in Northeast China, Sci. Total Environ., 710, 136304, https://doi.org/10.1016/j.scitotenv.2019.136304, 2020a.

Wang, X. L., Chancellor, G., Evenstad, J., Farnsworth, J. E., Hase, A., Olson, G. M., Sreenath, A., and Agarwal, J. K.: A Novel Optical Instrument for Estimating Size Segregated Aerosol Mass Concentration in Real Time, Aerosol Sci. Technol., 43, 939 - 950, 2009.

Wang, X. L., Zhou, H., Arnott, W. P., Meyer, M. E., Taylor, S., Firouzkouhi, H., Moosmüller, H., Chow, J. C., and Watson, J. G.: Characterization of smoke for spacecraft fire safety, J. Aerosol Sci., 136, 36-47, https://doi.org/10.1016/j.jaerosci.2019.06.004, 2019.

Wang, X. L., Zhou, H., Arnott, W. P., Meyer, M. E., Taylor, S., Firouzkouhi, H., Moosmüller, H., Chow, J. C., and Watson, J. G.: Evaluation of Gas and Particle Sensors for Detecting Spacecraft-Relevant Fire Emissions Fire Saf. J., 113, 1-12, https://doi.org/10.1016/j.firesaf.2020.102977, 2020b.

Wasson, S. J., Linak, W. P., Gullett, B. K., King, C. J., Touati, A., Huggins, F. E., Chen, Y., Shah, N., and Huffman, G. P.: Emissions of Chromium, Copper, Arsenic, and PCDDs/Fs from Open Burning of CCA-Treated Wood, Environ. Sci. Technol., 39, 8865-8876, 10.1021/es050891g, 2005.

Wesolek, D. and Kozlowski, R.: Toxic gaseous products of thermal decomposition and combustion of natural and synthetic fabrics with and without flame retardant, Fire Mater., 26, 215-224, 10.1002/fam.800, 2002.

Wiedinmyer, C., Yokelson, R. J., and Gullett, B. K.: Global Emissions of Trace Gases, Particulate Matter, and Hazardous Air Pollutants from Open Burning of Domestic Waste, Environ. Sci. Technol., 48, 9523-9530, 10.1021/es502250z, 2014.

Williams, M., Gower, R., Green, J., Whitebread, E., Lenkiewicz, Z., and Schröder, P.: No time to waste: Tackling the plastic pollution crisis before it's too late, Tearfund, London, UK, 2019.

Wilson, D. C. and Velis, C. A.: Waste management – still a global challenge in the 21st century: An evidence-based call for action, Waste Management & Research, 33, 1049-1051, 10.1177/0734242X15616055, 2015.

Wilson, D. C., Rodic, L., Modak, P., Soos, R., Carpintero, A., Velis, K., Iyer, M., and Simonett, O.: Global waste management outlook, United Nations Environment Programme (UNEP)2015.

Wu, D., Li, Q., Shang, X., Liang, Y., Ding, X., Sun, H., Li, S., Wang, S., Chen, Y., and Chen, J.: Commodity plastic burning as a source of inhaled toxic aerosols, J. Hazard. Mater., 416, 125820, https://doi.org/10.1016/j.jhazmat.2021.125820, 2021.

Xiu, M., Stevanovic, S., Rahman, M. M., Pourkhesalian, A. M., Morawska, L., and Thai, P. K.: Emissions of particulate matter, carbon monoxide and nitrogen oxides from the residential burning of waste paper briquettes and other fuels, Environ. Res., 167, 536-543, https://doi.org/10.1016/j.envres.2018.08.008, 2018.

Yokelson, R. J., Griffith, D. W. T., and Ward, D. E.: Open-path Fourier transform infrared studies of large-scale laboratory biomass fires, Journal of Geophysical Research: Atmospheres, 101, 21067-21080, 10.1029/96jd01800, 1996.

Yokelson, R. J., Burling, I. R., Gilman, J. B., Warneke, C., Stockwell, C. E., de Gouw, J., Akagi, S. K., Urbanski, S. P., Veres, P., Roberts, J. M., Kuster, W. C., Reardon, J., Griffith, D. W. T., Johnson, T. J., Hosseini, S., Miller, J. W., Cocker Iii, D. R., Jung, H., and Weise, D. R.: Coupling field and laboratory measurements to estimate the emission factors of identified and unidentified trace gases for prescribed fires, Atmos. Chem. Phys., 13, 89-116, 10.5194/acp-13-89-2013, 2013.

Yokelson, R. J., Crounse, J. D., DeCarlo, P. F., Karl, T., Urbanski, S., Atlas, E., Campos, T., Shinozuka, Y., Kapustin, V., Clarke, A. D., Weinheimer, A., Knapp, D. J., Montzka, D. D., Holloway, J., Weibring, P., Flocke, F., Zheng, W., Toohey, D., Wennberg, P. O., Wiedinmyer, C., Mauldin, L., Fried, A., Richter, D., Walega, J., Jimenez, J. L., Adachi, K., Buseck, P. R., Hall, S. R., and Shetter, R.: Emissions from biomass burning in the Yucatan, Atmos. Chem. Phys., 9, 5785-5812, 10.5194/acp-9-5785-2009, 2009.

Supplementary Materials

Characterization of Gas and Particle Emissions from Open Burning of Household Solid Waste

Xiaoliang Wang[1], Hatef Firouzkouhi[1], Judith C. Chow[1], John G. Watson[1], Warren Carter[2], Alexandra S.M. De Vos[2]

[1] Division of Atmospheric Sciences, Desert Research Institute, Reno, NV 89512, U.S.A.
[2] SASOL Research and Technology, Sasolburg, South Africa

Correspondence to: Xiaoliang Wang (xiaoliang.wang@dri.edu)

S1. Supplementary Tables

Table S1: Moisture contents of waste materials.

Material	Moisture (% of dry mass)
Paper	26.5
Leather/Rubber	0.52
Textile	6.9
Plastic bottles	0.54
Plastic bags	0.54
Vegetation	16.5
Food discards	34.7
Combined	8.52

Table S2: Major elemental compositions (mean ± standard deviation of three samples) of waste materials tested in this study and the carbon content assumed for IPCC (2006) emission estimates.

Material	C (%)	H (%)	N (%)	S (%)	O (%)	Other Elements (%)	C% in IPCC (2006)
Paper	44.10 ± 2.82	5.69 ± 0.84	0.68 ± 0.19	0.00 ± 0.00	44.08 ± 0.26	5.45 ± 3.64	46 (42–50)
Leather/Rubber	32.91 ± 0.07	2.88 ± 0.01	0.66 ± 0.00	0.16 ± 0.01	23.64 ± 0.27	39.76 ± 0.52	67
Textile	47.81 ± 3.50	5.84 ± 0.81	7.71 ± 1.11	0.71 ± 0.31	33.62 ± 2.63	4.32 ± 2.39	50 (25–50)
Plastic bottles	63.72 ± 5.36	5.10 ± 0.23	0.41 ± 0.09	0.00 ± 0.00	22.77 ± 2.35	8.00 ± 4.76	75 (67–85)
Plastic bags	84.42 ± 1.80	12.62 ± 0.82	0.20 ± 0.01	0.00 ± 0.00	2.78 ± 0.08	2.76 ± 4.90	
Vegetation	44.60 ± 1.10	5.32 ± 0.87	0.86 ± 0.11	0.00 ± 0.00	42.02 ± 1.65	7.20 ± 2.43	49 (45–55)
Food discards	34.78 ± 2.67	5.51 ± 0.43	3.66 ± 0.09	0.00 ± 0.00	41.43 ± 2.27	14.62 ± 3.68	38 (20–50)
Combined	41.06 ± 0.94	4.62 ± 0.70	1.50 ± 0.14	0.00 ± 0.00	21.32 ± 2.25	31.50 ± 3.50	NA

Table S3: Ash fractions (mass ratio of ash to the original dry materials) and major elemental compositions (mean ± standard deviation of three samples) for tested waste materials.

Material	Ash Fraction (%)	Major Elemental Content			
		C (%)	H (%)	N (%)	S (%)
Paper	6.9 ± 1.6	7.11 ± 0.34	0.22 ± 0.03	0.00 ± 0.00	0.00 ± 0.00
Leather/rubber	58.0 ± 2.3	12.80 ± 0.20	1.07 ± 0.32	0.00 ± 0.00	0.00 ± 0.00
Textile	11.1 ± 1.4	9.14 ± 1.01	0.37 ± 0.01	1.18 ± 0.32	0.00 ± 0.00
Plastic bottles	5.3 ± 3.1	77.44 ± 4.93	2.95 ± 0.30	0.11 ± 0.05	0.00 ± 0.00
Plastic bags	3.4 ± 1.0	10.99 ± 1.39	0.48 ± 0.05	0.21 ± 0.03	0.00 ± 0.00
Vegetation (0% mc*)	8.8 ± 2.6	6.21 ± 1.20	0.50 ± 0.08	0.18 ± 0.02	0.00 ± 0.00
Vegetation (20% mc*)	8.3 ± 0.4				
Vegetation (50% mc*)	7.5 ± 0.0				
Food discard	2.1 ± 0.5	41.04 ± 0.53	1.77 ± 0.04	3.23 ± 0.06	0.00 ± 0.00
Combined	19.9 ± 1.9	2.36 ± 0.93	0.31 ± 0.10	0.04 ± 0.06	0.00 ± 0.00

*mc: fuel moisture content. Elemental compositions for vegetations with 20% and 50% moisture content are assumed to be the same as that with 0% moisture content.

Table S4: Gas and particle measurement instruments for the combustion experiments.

Make/Model	Equipment Type and Operating Principle	Measurement Range	Data Rate
Li-Cor Model 840A CO_2 Analyzer	CO_2 analyzer by non-dispersive infrared (NDIR)	0–20000 ppm	1 s
Thermo 48i CO Analyzer	CO analyzer by gas filter correlation infrared absorbance	0–400 ppm	1 s
Thermo 43i SO_2 Analyzer	SO_2 analyzer by pulsed fluorescence	0–10 ppm	1 s
Testo Model 350 XL Emission Analyzer	CO (electrochemical) CO_2 (nondispersive infrared) NO (electrochemical) NO_2 (electrochemical) SO_2 (electrochemical) O_2 (electrochemical) Temperature Gauge Pressure	0–500 ppm 0–50% vol 0–300 ppm 0–500 ppm 0–5,000 ppm 0–25% vol -40–1200 °C -40–40 hPa	1 s
Horiba Model APNA-360 NO/ NO_2 Analyzer	NO, NO_2, and NO_x by chemiluminescence	0–1 ppm	1 s
TSI Model 8534 DustTrak DRX Aerosol Monitor	PM_1, $PM_{2.5}$, PM_4, PM_{10}, and PM_{15} by light scattering	0–400 mg m^{-3}	1 s
Dekati ELPI+[a]	Particle size distribution	0.006–10 µm	0.1 s
DMT PASS-3 Soot Spectrometer[a]	Light absorption by photoacoustic spectrometry and light scattering by integrated nephelometry at 3 wavelengths: 405, 532, and 781 nm	Absorption (2-s average): 3 Mm^{-1} @781nm, 10 Mm^{-1} (@ 532 and 405 nm	2 s
DRI Multi-Channel Low-volume Filter Sampler	Four filter channels to collect $PM_{2.5}$ for mass and future chemical analysis, as well as one Teflon filter for PM_{10} mass	Flow: 5 L min^{-1} each channel	30–120 min integrated

[a]Data from ELPI+ and PASS-3 are not included in this paper but will be reported in future publications.

Table S5: Comparison of measured and calculated emission factors for combined materials.

Combined Materials	Emission Factor (g kg^{-1} fuel)							
	CO_2	CO	NO (as NO_2)	NO_2	NO_x (as NO_2)	SO_2	$PM_{2.5}$	PM_{10}
Measured	1417	31.6	1.80	0.61	2.41	0.95	6.86	7.26
Calculated	1499	48.8	1.8	0.7	2.5	0.6	49.5	53.8
Relative Difference*	6%	54%	0%	8%	2%	-39%	621%	642%

*$Relative\ Difference = (Calculated - Measured)/Measured$

S2. Supplementary Figures

30

Figure S1: Photographs of household solid waste materials used in this study.

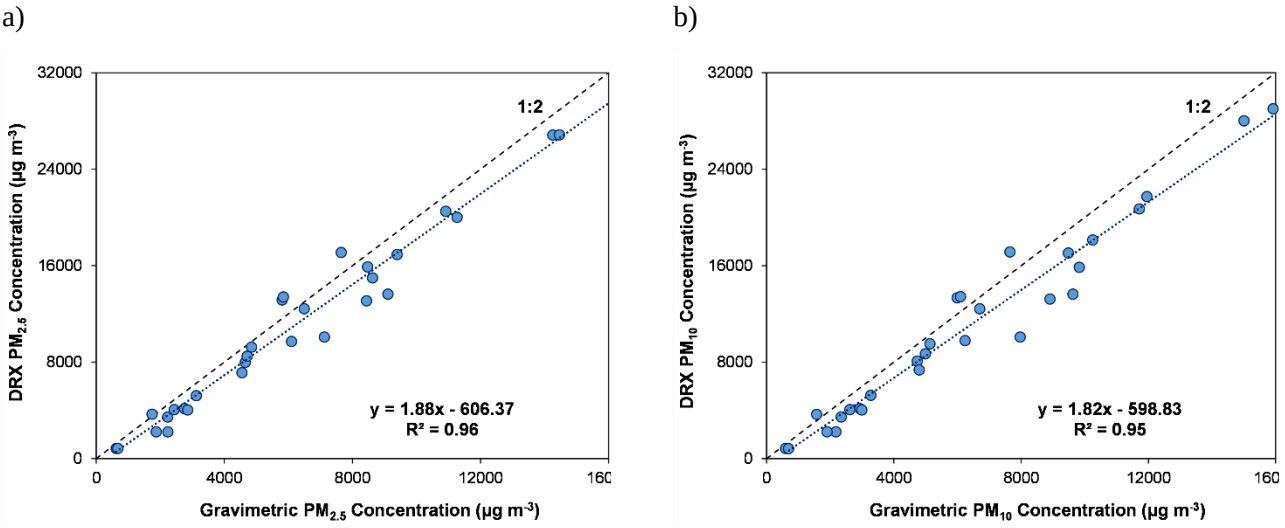

Figure S2: Comparisons of: a) $PM_{2.5}$ and b) PM_{10} mass concentrations by DRX and by gravimetry.

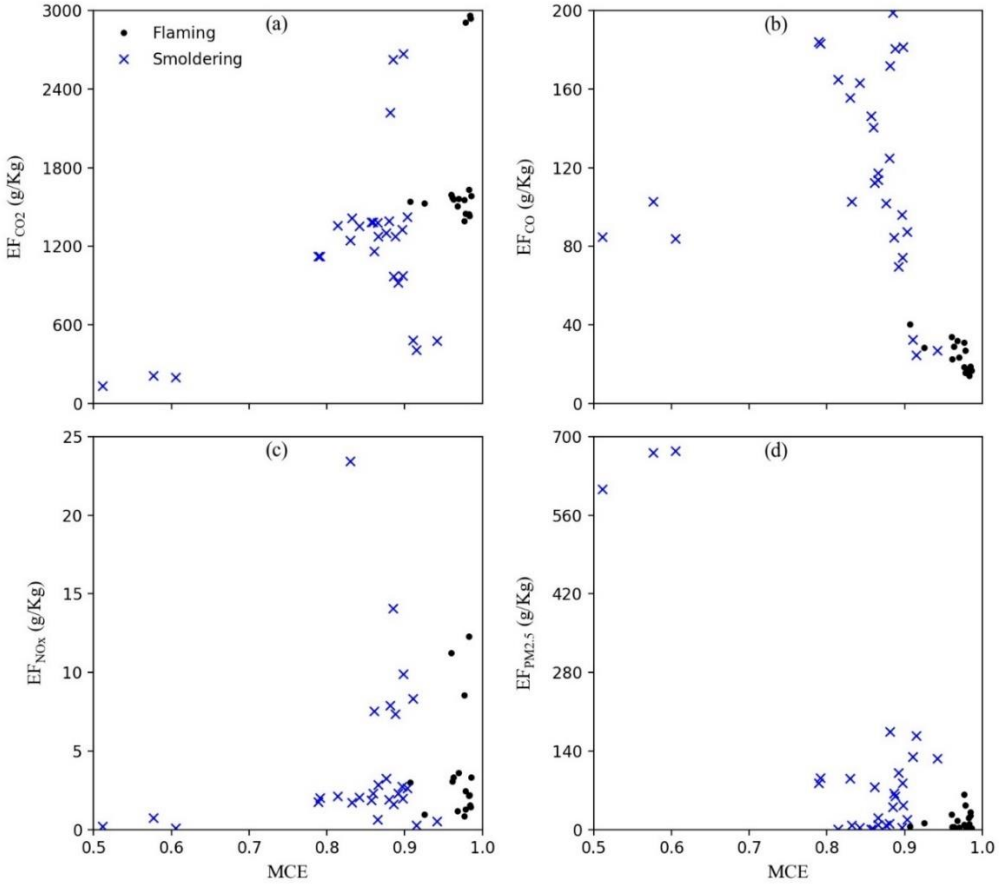

Figure S3: Flaming and smoldering emission factors vs MCE for: (a) CO_2, (b) CO, (c) NO_x (as NO_2), and (d) $PM_{2.5}$ for all fuels.

S3 Air Pollutant Emission Evolution during Combustion

This section presents time series plots of criteria pollutant emissions as a function of time during the burns. Time series plots provide insights into combustion behaviors of different waste materials.

S3.1 Paper

The paper burning experiment utilized 10 g of dried paper, moisturized to 26.5% water content. The prepared material was then placed in a heated ceramic crucible inside the burn chamber and was subjected to exhaust from a heat gun. The material was ignited after ~40 seconds, as indicated by the left boundary of the shaded area in Figure S4~~Figure S4~~, and the paper started flaming with increasing pollutant concentrations. Pollutants related to more complete combustion and higher combustion temperatures (i.e., CO_2, SO_2, NO, and NO_2) increased faster than those related to incomplete combustion (i.e., CO and $PM_{2.5}$). The MCE was high (>0.93). As the paper was consumed, the fire became smaller, and CO_2, SO_2, NO, and NO_2 concentrations decreased. There was also a period when flaming and smoldering emissions coexisted. Eventually, the visible flame died out and smoldering emissions took over (as indicated by the right boundary of the shaded area).

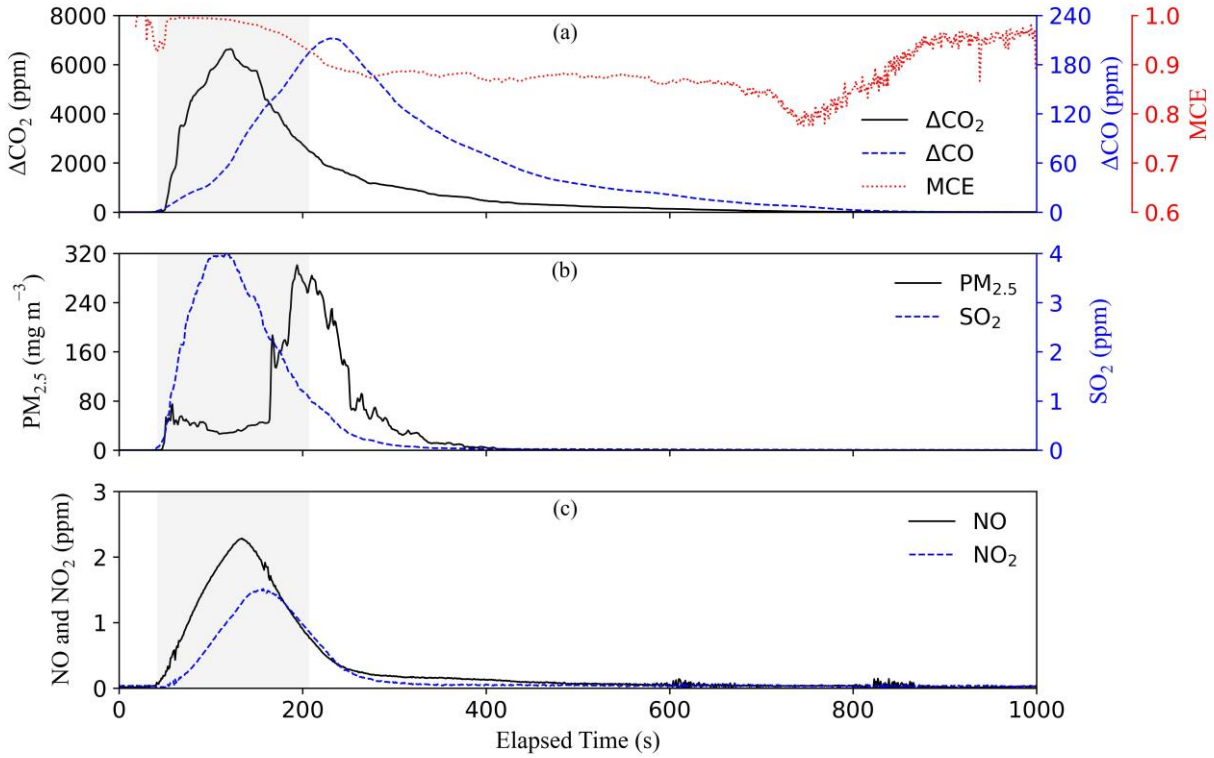

Figure S4: Time series of pollutant concentrations during a paper burning experiment. The shaded area indicates flaming stage.

During smoldering, CO_2, SO_2, NO, and NO_2 continued to decrease while CO and $PM_{2.5}$ concentrations reached their maxima and gradually decreased as the fuel was consumed. The MCE remained low during the smoldering stage. The higher MCE at the end of the experiment (after ~750 seconds) was an artifact due to CO concentrations being near background levels.

The test ended when all concentrations attained background levels. The heater was turned off and filters and ashes were collected for weighting and laboratory analysis. Figure S5~~Figure S5~~ shows the fuel and ashes at the end of the test. Filter deposits from the paper test are shown in Figure S6~~Figure S6~~, with the $PM_{2.5}$ and PM_{10} filters containing 1.69 and 1.78 mg PM mass, respectively. OC and EC were 55.1% and 6.6% of $PM_{2.5}$, respectively. The light yellow color of the filters indicates the presence of brown carbon - light absorbing particles at shorter visible wavelengths.

a) b)

Figure S5: Paper material in a heated- ceramic crucible: a) before burning and b) after burning.

Figure S6: Filters with PM collected from paper burning tests; from left to right: Teflon-membrane for $PM_{2.5}$, two Quartz filters in the middle for $PM_{2.5}$, and Teflon-membrane for PM_{10}.

S3.2 Leather/Rubber

The leather/rubber material was derived from a car floor mat. Unlike tires, this rubber material does not flame, but it pyrolyzes, decays, and evaporates when heated, similar to smoldering for the other fuels. Three grams of chopped rubber material moisturized to 0.52% was placed in the ceramic crucible (Figure S7~~Figure S7~~a). The test started by setting the heater temperature to 450 °C; after ~200 seconds, the fuel reached ~100 °C and smoldering started. As shown in Figure S8~~Figure S8~~, all pollutants gradually increased, except for NO_x that forms at high temperatures. CO and CO_2 concentrations were low – almost the lowest among all tests, while $PM_{2.5}$ concentrations were high. The rubber tests yielded the second highest (after plastic bottles) emission factors for PM. Almost all rubber was consumed after ~26 minutes, and all pollutants returned to background levels. The MCE was ~92% during most part of the smoldering.

By the end of the test, more than half of the fuel remained as ash (Figure S7~~Figure S7~~b). Rubber had the most unburned residue among all tested waste materials (Table S3~~Table S3~~). This is consistent with the high fraction of elements other than C, H, N, S, and O in Table S2~~Table S2~~. High amounts of ash (~58%) play an important role in EF calculation according to Eq. (2).

Figure S9~~Figure S9~~ shows the filters from this test, which look like the blank filter. However, each $PM_{2.5}$ and PM_{10} filter contained 2.36 and 2.47 mg PM mass, respectively, indicating the lack of visible light absorbing components, as also evidenced by the low EC (0.2% of $PM_{2.5}$) loadings.

a) b)

Figure S7: Rubber material in a heated ceramic crucible: a) before burning and b) after burning.

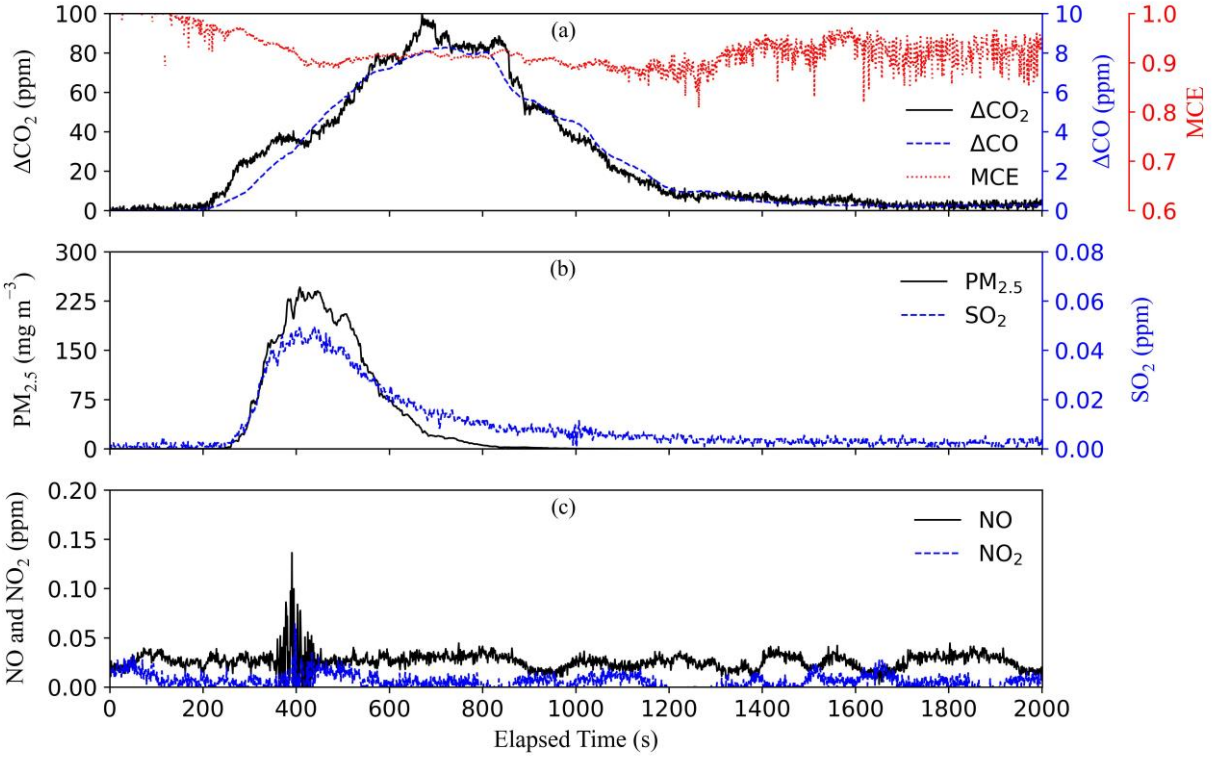

Figure S8: Concentration time series during a rubber burning experiment.

Figure S9: Filters with PM collected from rubber burning tests; from left to right: Teflon-membrane for $PM_{2.5}$, two Quartz filters in the middle for $PM_{2.5}$, and Teflon-membrane for PM_{10}.

S3.3 Textiles

Figure S10~~Figure S10~~a shows 5 g of the prepared textile material that was moisturized to 6.9% water content. Combustion showed two flaming stages caused by the different textile types in the fuel mix. One part of the fuel started to flame right after ignition by the heat gun (first shaded area). After the more flammable materials were consumed, the fire smoldered for ~140s, then the less flammable materials started to flame (second shaded area). Although the first flaming stage had higher CO_2, SO_2, and NO_x emissions, the second flaming phase had higher CO and PM emissions. The mean MCE for the second flaming stage was lower than that for the first one. Among all tested materials, the textiles had the highest emission factors for NO_x and SO_2.

a) b)

Figure S10: Textile material in a heated ceramic crucible: a) before burning and b) after burning.

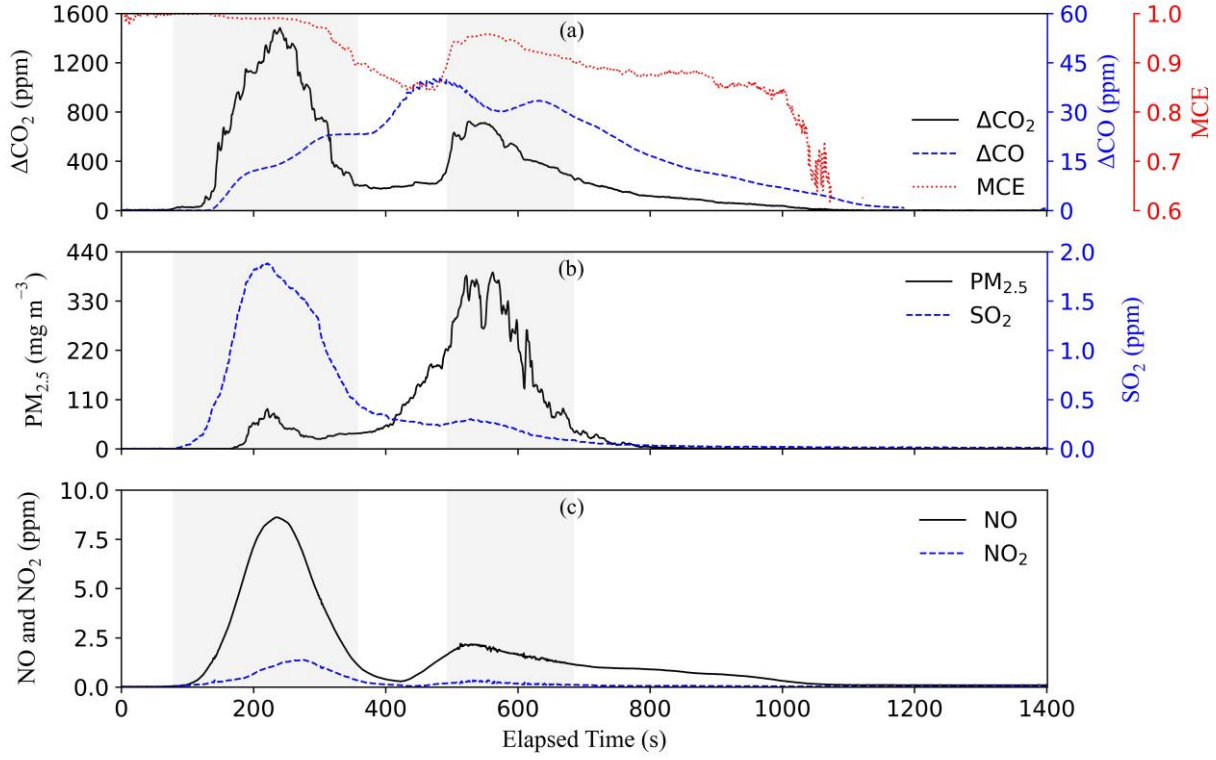

Figure S11: Time series of concentrations during a textile burning experiment. The shaded areas indicate flaming stages.

Textile ash, Figure S10~~Figure S10~~b, was ~11% of the fuel total weight. The collected filters are depicted in Figure S12~~Figure S12~~, with each $PM_{2.5}$ and PM_{10} filter containing 1.16 and 1.18 mg of PM mass, respectively. The PM deposits were dark grey, consistent with abundant EC levels (15% of $PM_{2.5}$). The dark color of indicates that the textile smoke has a significant light absorption effect.

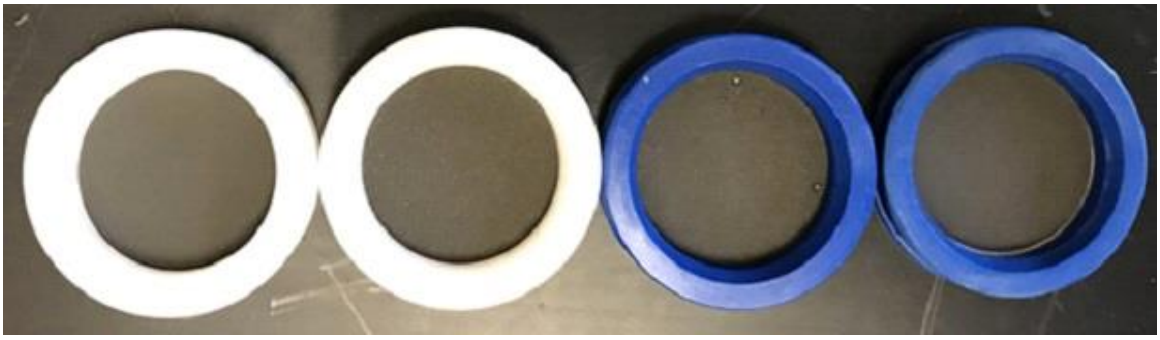

Figure S12: Filters with PM collected from a textile burning; from left to right: Teflon-membrane for $PM_{2.5}$, two Quartz filters in the middle for $PM_{2.5}$, and Teflon-membrane for PM_{10}.

S3.4. Hard Plastic (Bottles)

Smoldering combustion of plastic bottles (hard plastic) generated high PM concentrations that clogged filters and contaminated some test instruments during initial trial burns. Only 0.5 g of the prepared material, as shown in Figure S13~~Figure S13~~a, was used for subsequent burns. The moisture content of the plastic bottles was 0.54%.

a) b)

Figure S13: Hard plastic (bottle) material in a heated ceramic crucible: a) before burning and b) after burning.

Concentration time series plots are shown in Figure S14~~Figure S14~~. The bottles did not flame and only smoldered, generating low CO_2 and CO emissions. However, PM emissions were the highest among all the waste materials. The strong plastic odor and light-yellow colored sticky particles were likely formed from condensation of semi-volatile thermal decomposition products, such as carboxylic acids and hydroxyl esters including phthalates ~~re-condensation of evaporated plastic molecules~~(Sovová et al., 2008; Holland and Hay, 2002). The MCE was only ~0.6 during most of the burn, indicating low combustion efficiencies. The low combustion temperature and low nitrogen content in the fuel (Table S2~~Table S2~~) resulted in low NO_x emissions.

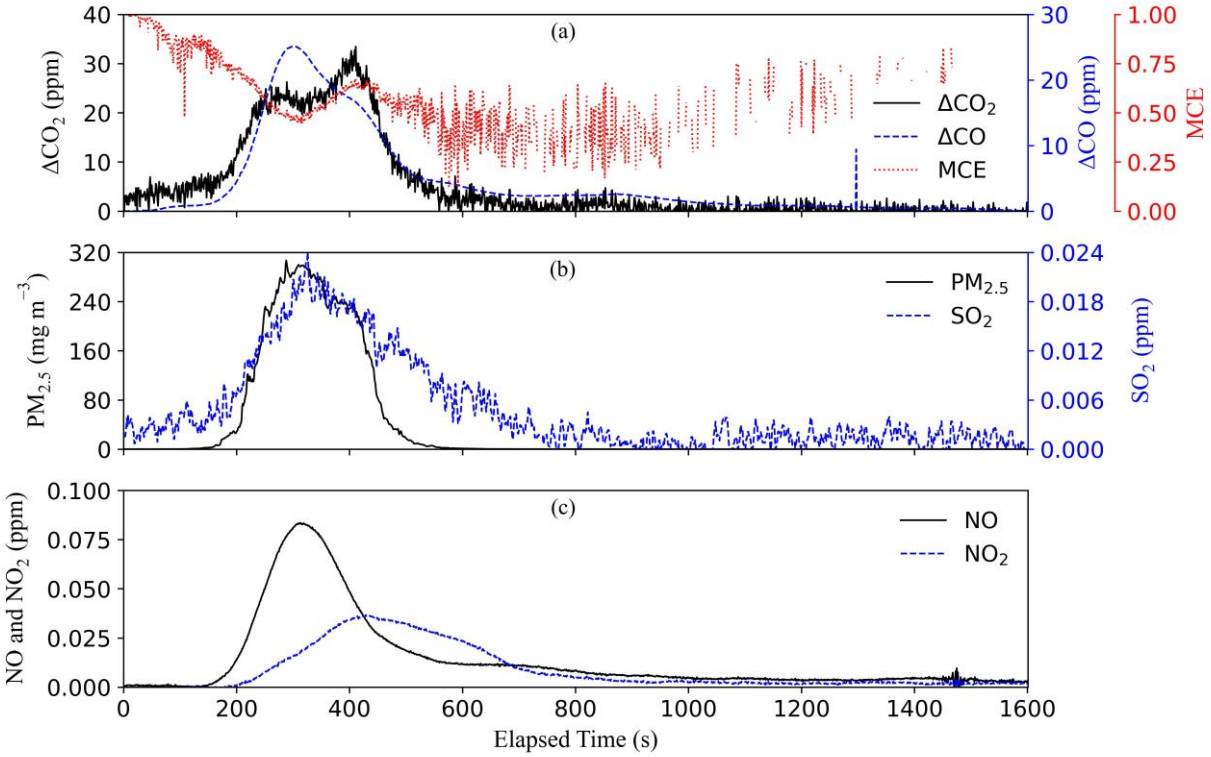

Figure S14: Time series of concentrations during a hard plastic (bottles) burning experiment.

Almost all of the fuel was consumed, and only ~5% ash remained as illustrated in Figure S13~~Figure S13~~b. Strong smoldering was observed when the heater temperature exceeded 350 ˚C. The PM deposit appearances (Figure S15~~Figure S15~~) were similar to those of blank filters, although $PM_{2.5}$ and PM_{10} filters contained 2.49 and 2.72 mg PM mass, respectively, indicating the smoke was mainly composed of non-light absorbing PM composition at visible wavelengths with low amounts of elemental carbon (<1% of $PM_{2.5}$).

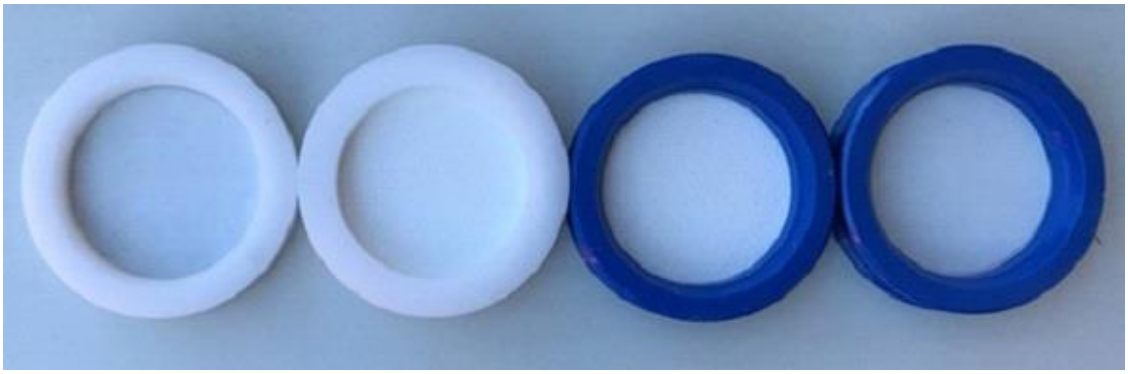

Figure S15: Filters with PM collected from hard plastic (bottle) burning; from left to right: Teflon-membrane for $PM_{2.5}$, two Quartz filters in the middle for $PM_{2.5}$, and Teflon-membrane for PM_{10}.

S3.5 Soft Plastic (Bags)

Soft plastic materials - mostly composed of shopping bags, packaging bags, bubble wrap, and cellophanes - form a large portion of the household wastes. Plastic waste is the second most common part of South African municipal solid waste (Fig. 1). It is estimated that plastic materials production and will double in next 20 years. Plastics are mostly used in packaging or construction (Lebreton and Andrady, 2019). In this test, 5 g of the material shown in Figure S16~~Figure S16~~a was prepared with 0.54% moisture content.

In contrast to the smoldering-only combustion of hard plastic (bottles), flaming dominated soft plastic combustion (Figure S17~~Figure S17~~). The MCE was high (> 0.94) during most parts of burn, indicating high combustion efficiencies. Soft plastic bags had the highest and lowest emission factors for CO_2 and CO, respectively, consistent with their high C and H contents (Table S2~~Table S2~~). A small amount of ash (3.4%) remained in the crucible (Figure S16~~Figure S16~~b). PM deposits on filters were black (Figure S18~~Figure S18~~) - the darkest among all samples, with $PM_{2.5}$ and PM_{10} filters containing 1.51 and 1.59 mg PM mass, respectively. These emissions had the highest EC abundances (70% of $PM_{2.5}$).

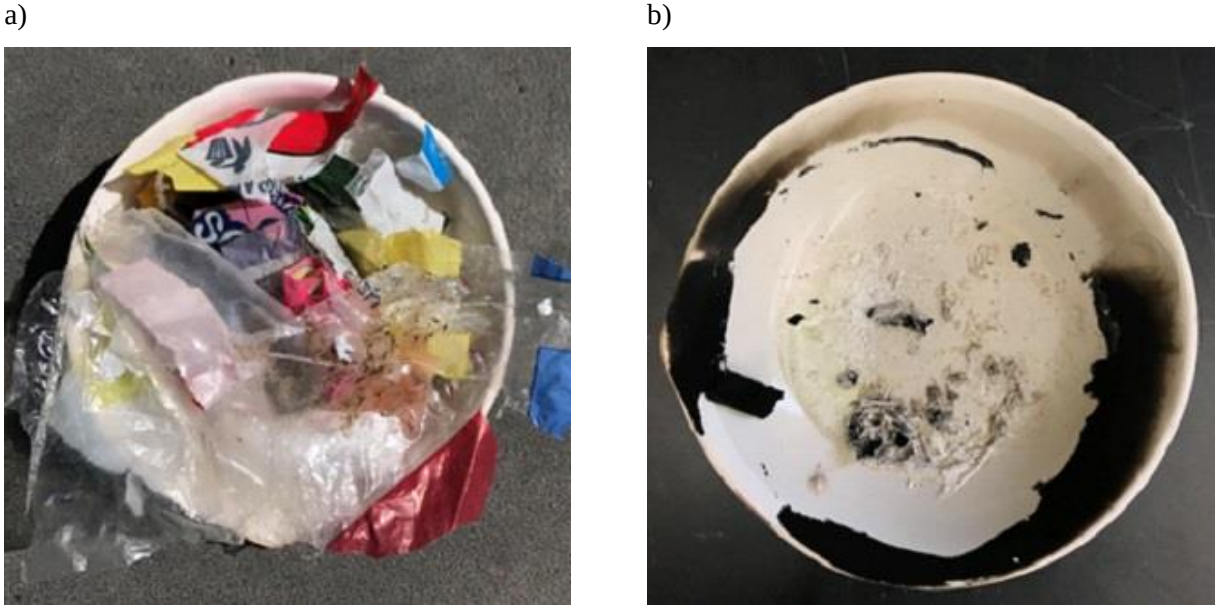

Figure S16: Soft plastic (bags) material in a heated ceramic crucible: a) before burning and b) after burning.

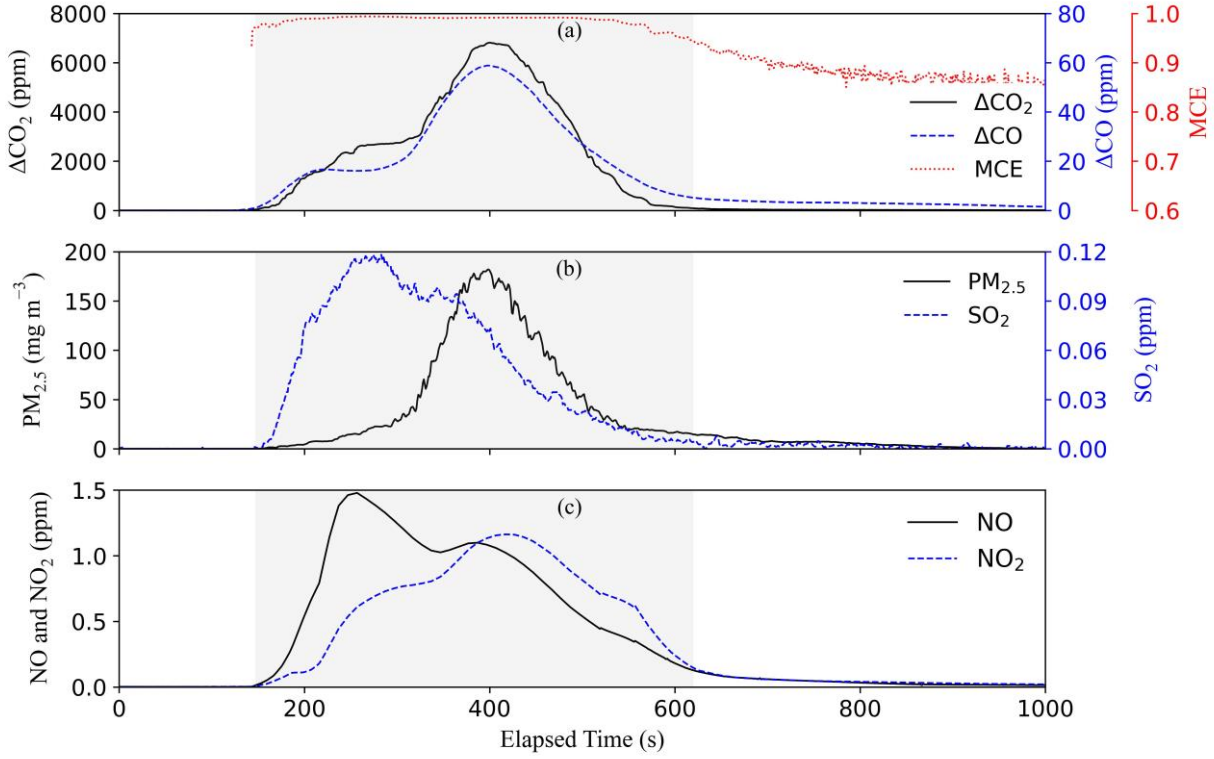

Figure S17: Time series of emissions during a soft plastic (bags) burning experiment. The shaded area indicates flaming stage.

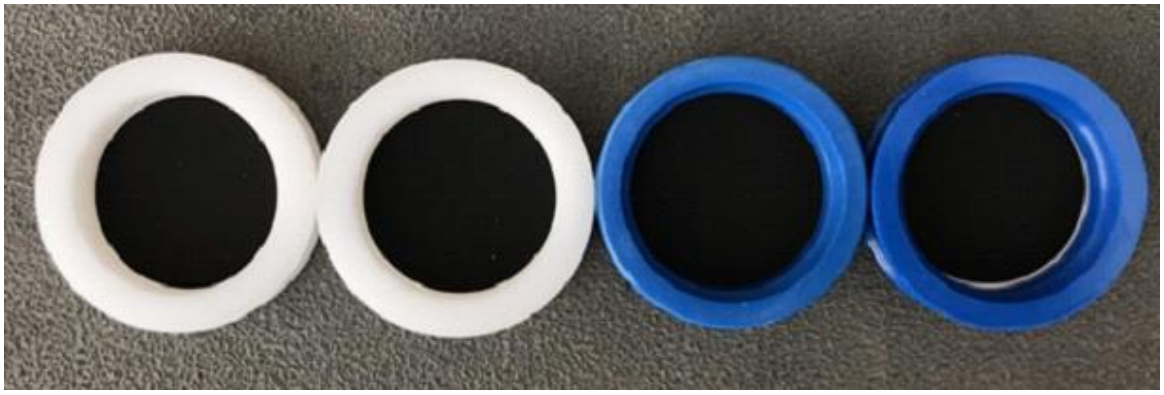

Figure S18: Filters with PM collected from a soft plastic (bags) burning test; from left to right: Teflon-membrane for $PM_{2.5}$, two Quartz filters in the middle for $PM_{2.5}$, and Teflon-membrane for PM_{10}.

S3.6 Wood / Vegetation

For the vegetation burns, 10 g of the dry vegetation, 10 g with 20% moisture, and 2 g with 50% moisture contents were prepared (Figure S19~~Figure S19~~). Figure S20~~Figure S20~~, Figure S21~~Figure S21~~, and Figure S22~~Figure S22~~ show pollutant concentration time series for the different moisture contents. Burning behaviors between the 0% and 20% moisture contents were similar, except that the flaming started earlier for the 20% moisture content case (indicated by a smaller peak at the beginning of the test). Once the moisture evaporated upon heating, most of the fuel was consumed by flaming. The combustion behavior for the 50% moist vegetation was different. The fuel only smoldered, probably owing to water evaporation during heating; the fuel charred and did not flame. The damp vegetation emitted less CO_2, but higher levels of CO and PM. Different emission factors observed between vegetations with 50% and 0-20% moisture contents underline the importance of and also the challenges in obtaining representative fuel conditions for accurate real-world pollutant emissions. The MCEs for 0%, 20%, and 50% moisture content vegetation were ~0.92, ~0.9, and 0.8, respectively, indicating the role of the moisture in the combustion efficiency (Chen et al., 2010). At the end of the test, 7.5 to 8.8% of the fuel weight (Table S3~~Table S3~~) remained as ash, indicating that most of the fuel participated in the burn.

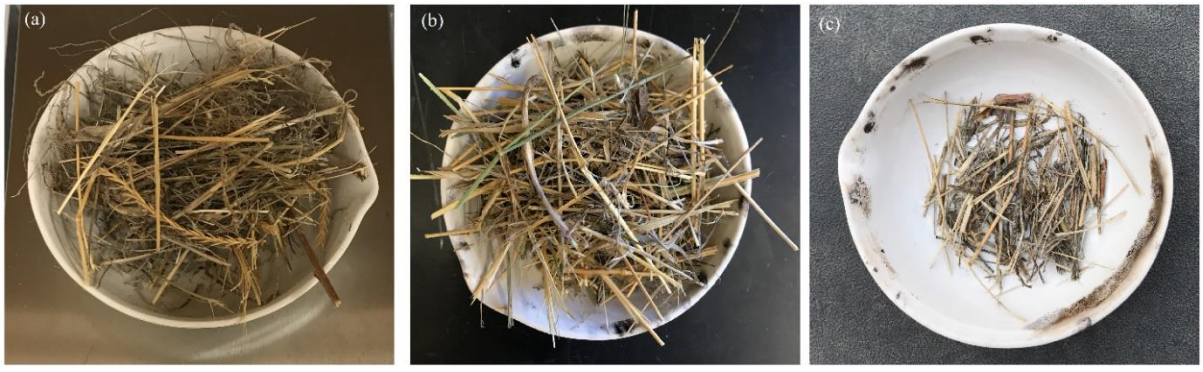

Figure S19: Vegetation material, in a heated ceramic crucible for: (a) dry, (b) 20%, and (c) 50% moisture content.

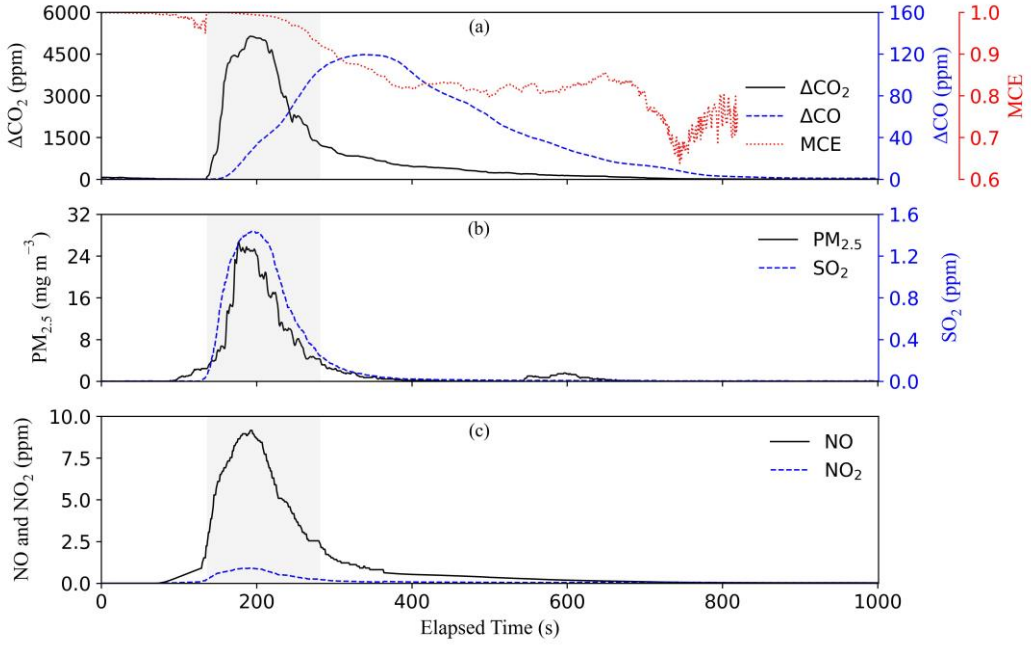

Figure S20: Time series of concentrations during a dry vegetation (0% moisture) burning experiment. The shaded area indicates the flaming stage.

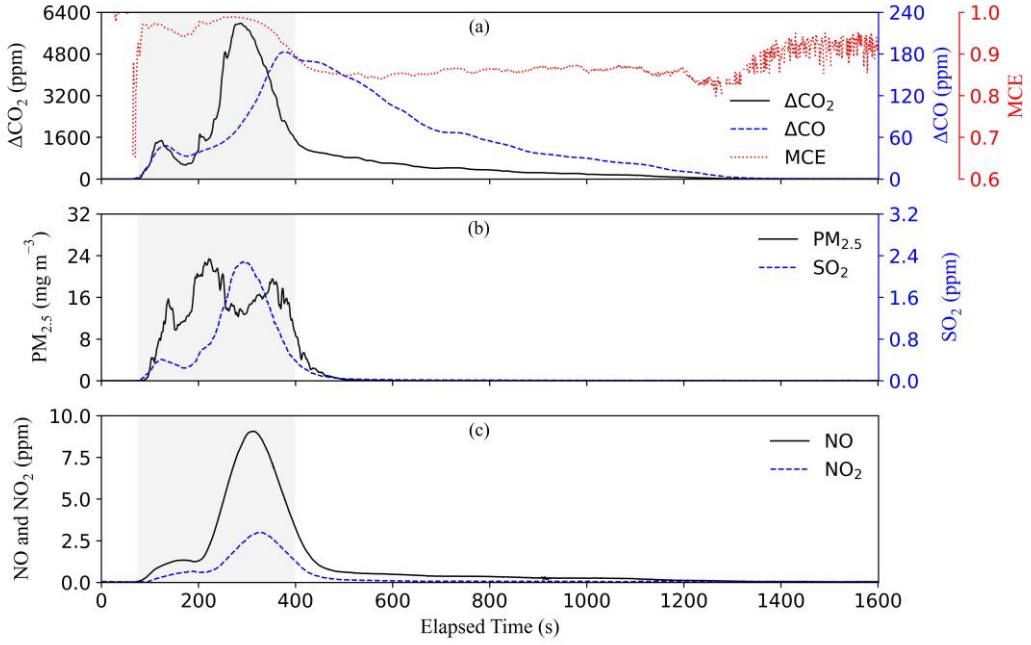

Figure S21: Time series of concentrations during a vegetation (20% moisture) burning experiment. The shaded area indicates flaming stage.

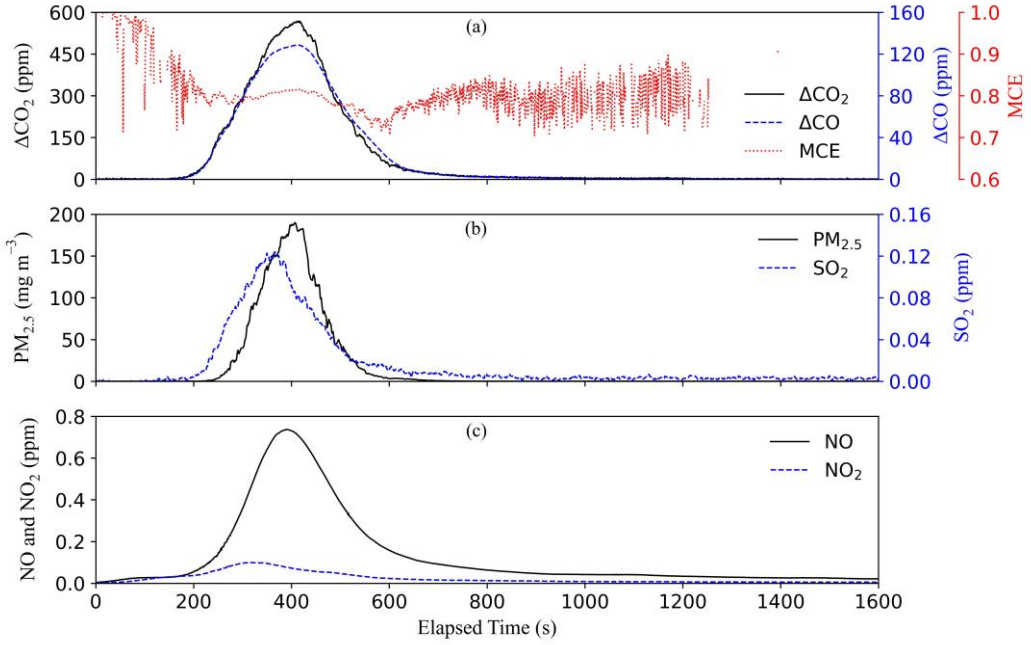

Figure S22: Time series of concentrations during a vegetation (50% moisture) burning experiment.

Figure S23: Vegetation ashes for: (a) dry, (b) 20%, and (c) 50% moisture contents.

Sampling filters from emissions of the vegetation with 0 and 20% moisture often look like blank filters; however, the 50% moisture fuel gave a pale yellow color (Figure S24~~Figure S24~~). The $PM_{2.5}$ and PM_{10} filter mass loadings are: 0.12 and 0.12 mg for dry fuel, 0.32 and 0.33 mg for 20% moist fuel, and 1.19 and 1.25 mg for 50% moist fuel, respectively. The EC abundance decreased from 9.3% of $PM_{2.5}$ for dry fuel, to 4.4% of $PM_{2.5}$ for 20% moist fuel, and to 2.7% of $PM_{2.5}$ for 50% moist fuel due to decreasing flaming and increasing smoldering as moisture content increased. Filters from the 50% moist fuel show a pale yellow color, indicating the presence of more brown carbon components in the smoldering smoke of this fuel.

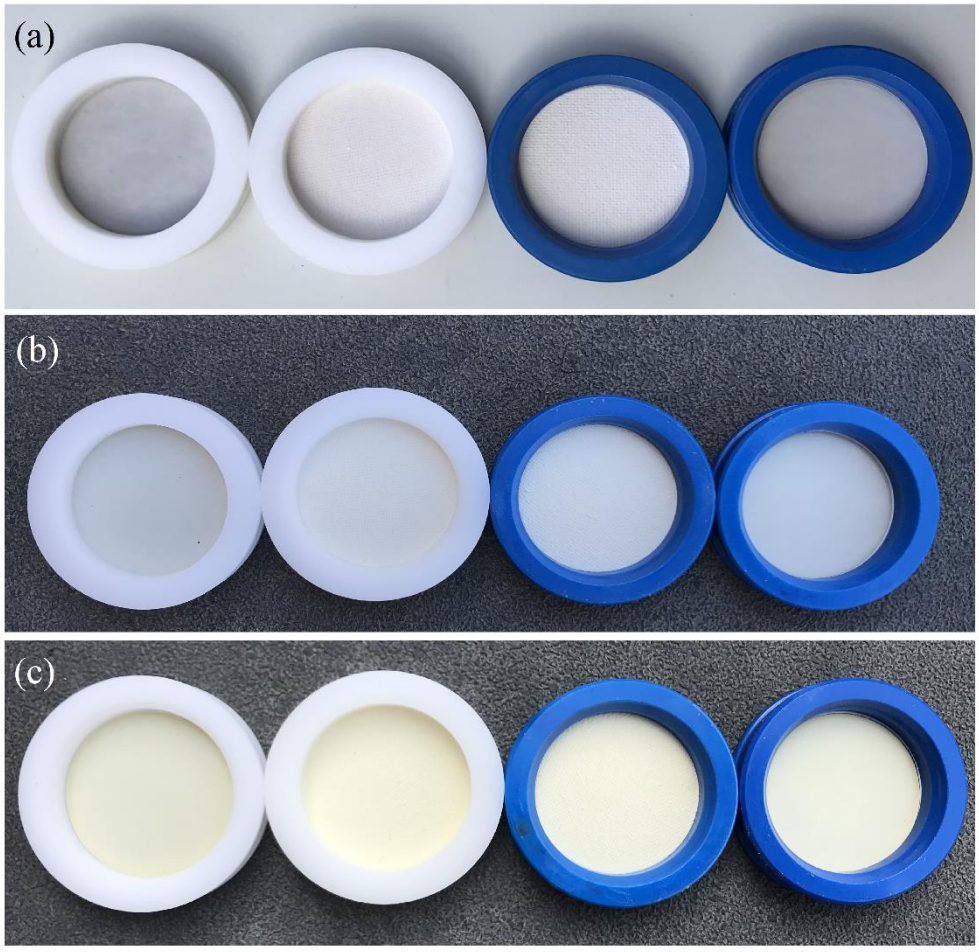

Figure S24: Filters with PM collected from three vegetation burning tests. (a): dry, (b): 20%, and (c): 50% water content; from left to right: Teflon-membrane for $PM_{2.5}$, two Quartz filters in the middle for $PM_{2.5}$, and Teflon-membrane for PM_{10}.

S3.7 Food Discards

As shown in Figure S25~~Figure S25~~a, food waste was represented by a mixture of bread, potato and banana peels, lettuce, cucumber, and tomato (Cronjé et al., 2018). In their natural state, food discards had a moisture content of 34.7% (Table S1~~Table S1~~), the highest among all tested waste materials. The time series for burning of food discards are shown in Figure S26~~Figure S26~~. Only smoldering was observed due to high moisture content, with low CO_2 and high CO and PM emissions. The MCE was ~0.90 during the most parts of the burn.

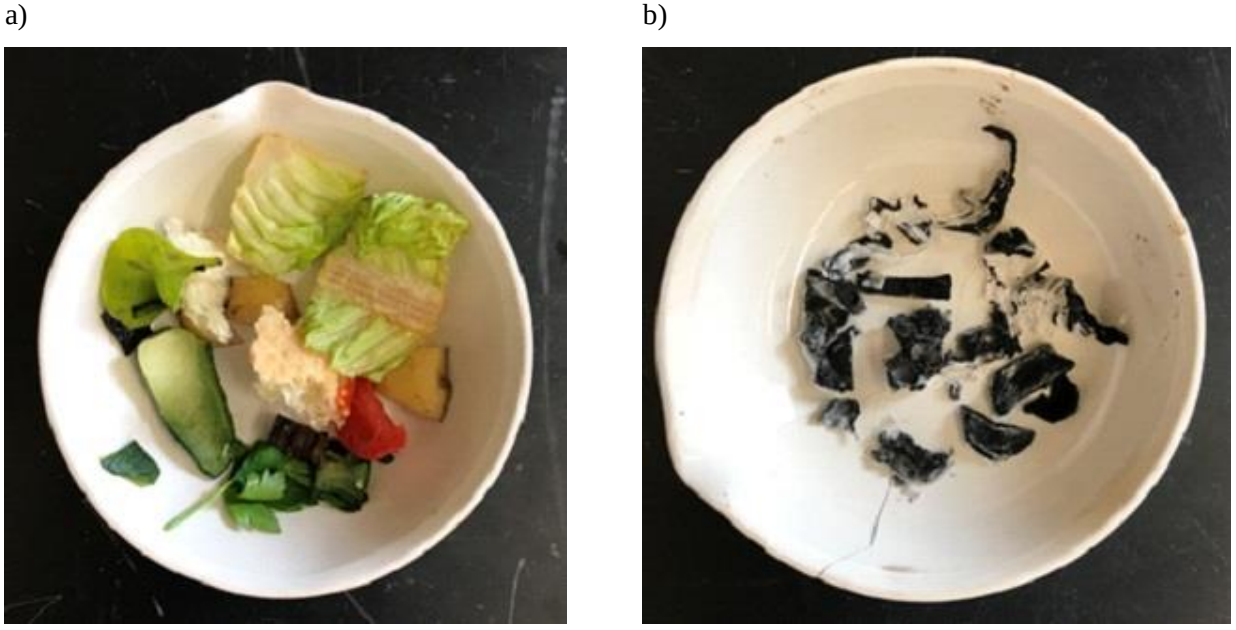

Figure S25: Food discard materials in a heated ceramic crucible: a) before burning and b) after burning.

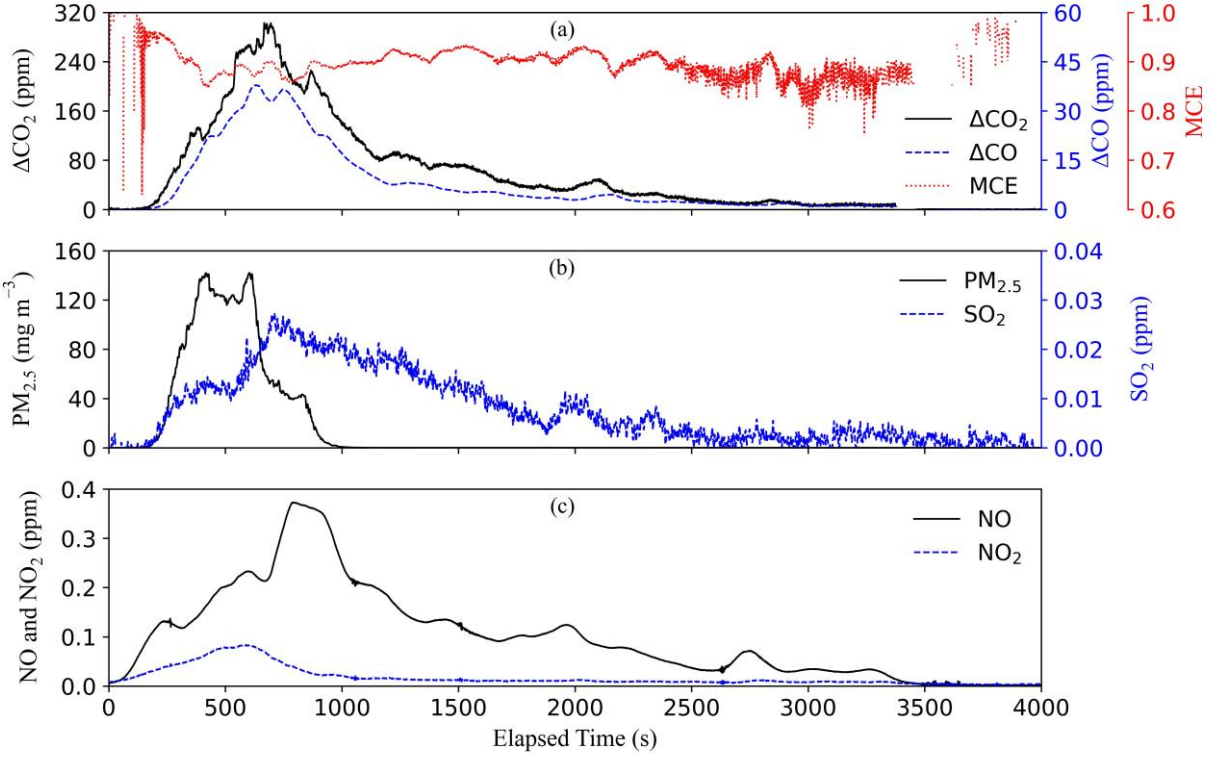

Figure S26. Time series of concentrations during a food discards burning experiment.

Due to their organic nature, food discards only had ~2% dry mass remaining as ash (Figure S25~~Figure S25~~b) after combustion, the lowest ash fraction among the fuels (Table S3~~Table S3~~). PM deposits on the filters are depicted in Figure S27~~Figure S27~~, with the $PM_{2.5}$ and PM_{10} filters containing 2.27 and 2.31 mg PM mass, respectively. OC and EC were 52.5% and 0.8% of $PM_{2.5}$, respectively. The yellow appearance of the filters indicates the presence of brown carbon compounds that absorb light at shorter visible wavelengths.

Figure S27: Filters with PM collected from food discards burning; from left to right: Teflon-membrane for $PM_{2.5}$, two Quartz filters in the middle for $PM_{2.5}$, and Teflon-membrane for PM_{10}.

S3.8 Combined Materials

The final tests involved a mixture from all waste categories, including ceramic, glass, and metals. Although ceramic, glass, and metal were not combustible at typical open burning temperatures, they were included to evaluate real-world combustion of a mixed waste stream. Based on the weight fraction of materials in the combined group (Fig. 1), 10 g of the fuel with 8.52% moisture content was prepared, as shown in Figure S28~~Figure S28~~a.

The combustion behavior of combined waste materials (Figure S29~~Figure S29~~) was similar to those of paper (Figure S4~~Figure S4~~) and dry vegetation (Figure S20~~Figure S20~~). Flaming was initiated in the most flammable materials such as paper and plastic bags, causing increased pollutant releases related to more complete combustion and higher combustion temperatures (i.e., CO_2, SO_2, NO, and NO_2). Peak concentrations of CO and PM appeared when the combustion transitioned from flaming to smoldering. The MCE for most of the burn period exceeded 0.90. After >5 minutes, the visible flame died out followed by the smoldering phase.

Figure S28~~Figure S28~~b shows that about 2 g (20% of dry mass) ash remained in the crucible; considering that glass, metal and ceramic did not contribute to the combustion, a high ash fraction was expected. PM deposits are illustrated in Figure S30~~Figure S30~~, with the $PM_{2.5}$ and PM_{10} filters containing 0.67 and 0.70 mg PM mass, respectively. The black color of the filters is due to abundant EC (48.1% of $PM_{2.5}$ mass), which has high light absorption efficiency for all wavelengths.

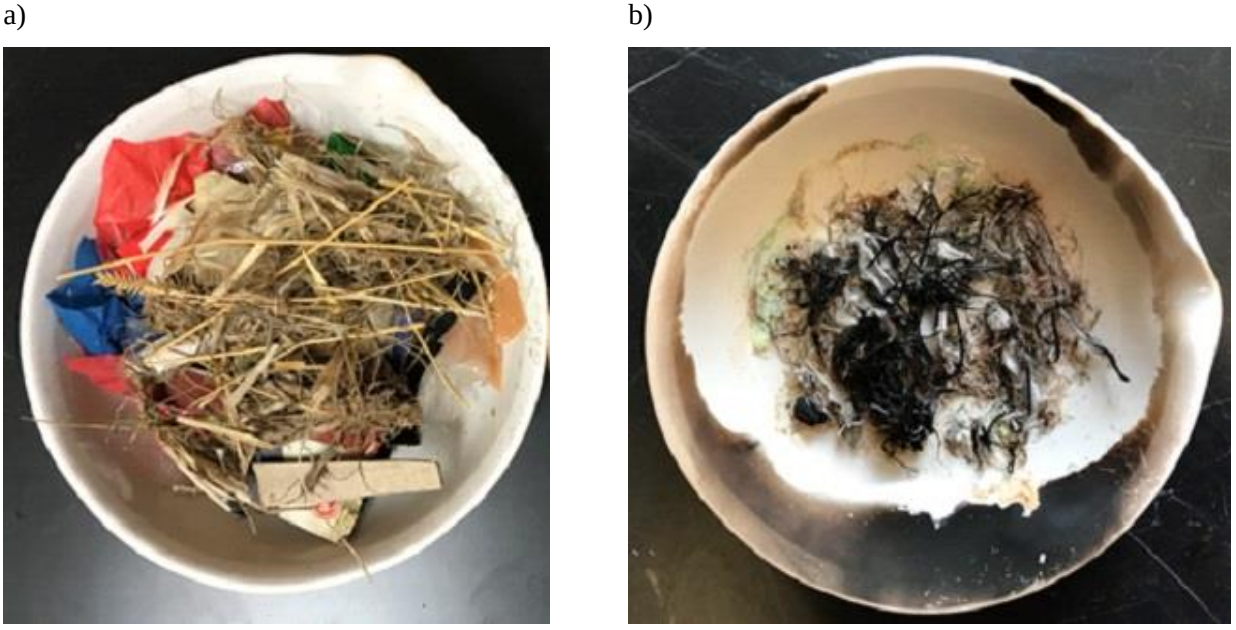

Figure S28: Combined materials in a heated ceramic crucible: a) before burning and b) after burning.

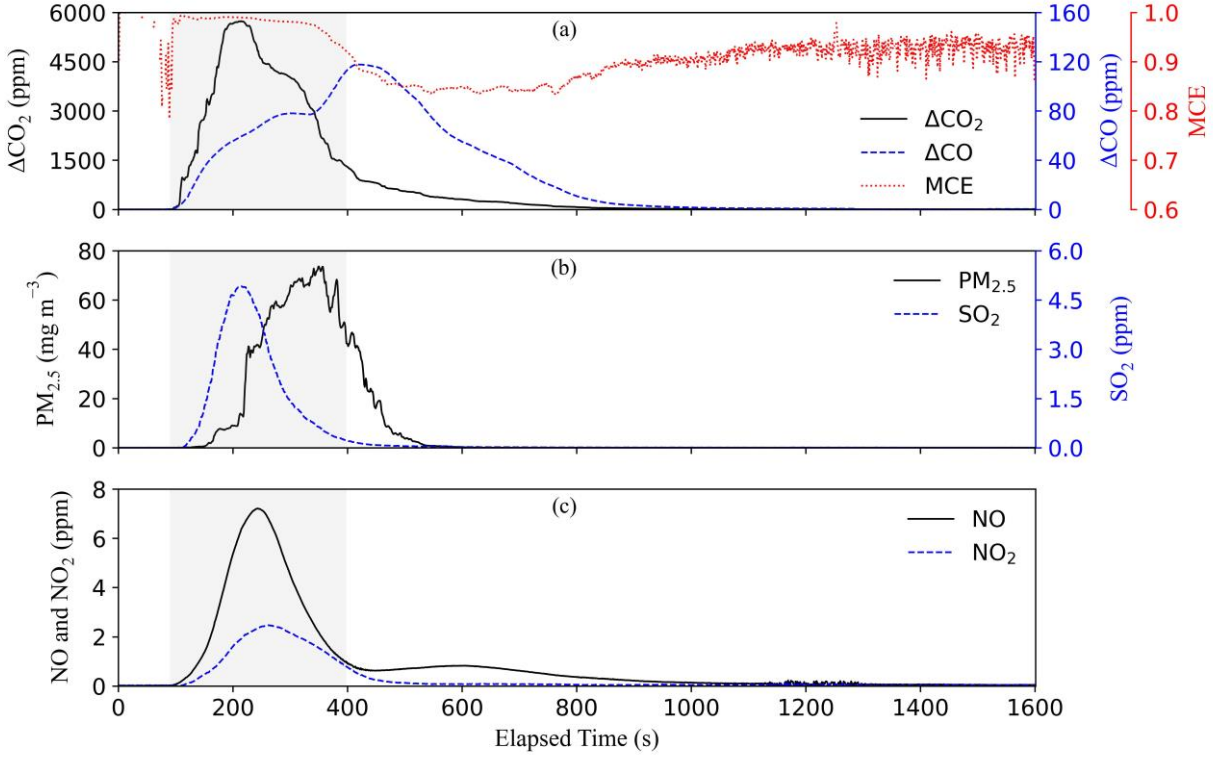

Figure S29: Time series of concentrations during combined waste burning experiment. The shaded area indicates flaming stage.

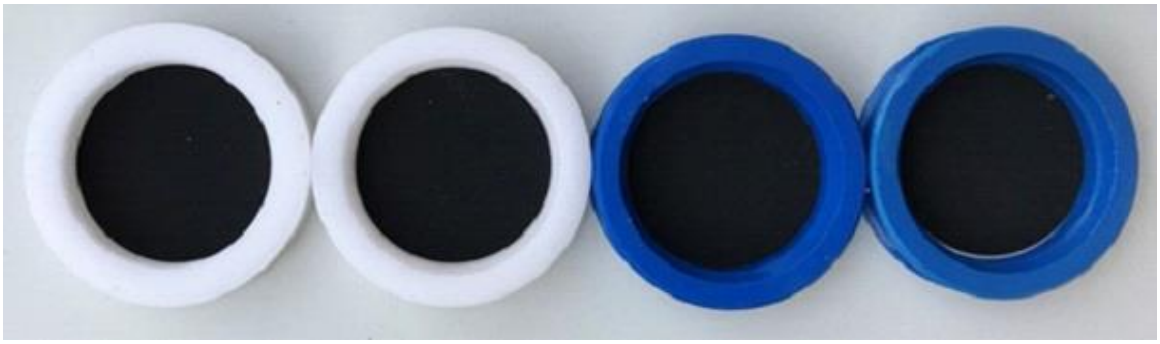

Figure S30: Filters with PM collected from a combined materials burning test; from left to right: Teflon-membrane for $PM_{2.5}$, two Quartz filters in the middle for $PM_{2.5}$, and Teflon-membrane for PM_{10}.